Flexible operation of a combined cycle cogeneration plant - A techno-economic assessment

Applied Energy 278 (2020) 115630

Contents lists available at ScienceDirect

Applied Energy

journal homepage: www.elsevier.com/locate/apenergy

Flexible operation of a combined cycle cogeneration plant – A techno-economic assessment

Johanna Beiron *, Rubén M. Montañés, Fredrik Normann, Filip Johnsson

Department of Space, Earth and Environment, Chalmers University of Technology, Gothenburg, Sweden

HIGHLIGHTS

- Process and optimization modeling for combined cycle flexibility assessment.
- Variable/controllable heat load or product mix more valuable than high ramp rate.
- Steam cycle heat-only operation is dispatched to reduce operational cost.
- Flexibility in heat load enables electricity-following operational strategies.
- Flexibility may give 16.5 M€/a for a 250 MW combined cycle depending on scenario.

ARTICLE INFO

Keywords:
Gas turbine combined cycle
Combined heat and power
District heating
Flexibility
Steam cycle
Process optimization

ABSTRACT

The need for flexibility in combined heat and power (CHP) plants is expected to increase due to the strong expansion of wind power in electricity systems. Cost-effective strategies to enhance the flexibility of CHP operation are therefore needed. This paper analyzes three types of flexibility measures for a combined cycle CHP plant and their relative impact on the plant operation and revenue. The types of flexibility are: operational flexibility of the fuel conversion system, product flexibility with variable plant product ratios (heat/electricity/primary frequency response), and thermal flexibility in a district heating network. A modeling framework consisting of steady-state and dynamic process simulation models and optimization model is developed to combine static, dynamic, technical and economic perspectives on flexibility. A reference plant serves as a basis for the process model development and validation, and an energy system model provides input profiles for future electricity price scenarios. The results indicate that product flexibility and thermal flexibility have the highest value for the cogeneration plant (up to 16.5 M€ increased revenue for a 250 MW_{el} plant), while operational flexibility (ramp rate) has a comparatively small impact (<1.4 M€). A wide load span and plant versatility, e.g. electricity and heat generating potential between 0 and 139% of nominal capacity, is beneficial in future energy system contexts, but has a marginal value in the current system. Electricity price volatility is a main driver that increases the value of flexibility and promotes operating strategies that follow the electricity price profile rather than the heat demand.

1. Introduction

Due to the increase of non-dispatchable power generation in energy systems, the flexibility of electricity systems will need to be enhanced to manage variability, maintain system stability and balance demand and supply [1,2]. Electricity system flexibility can be divided into four main categories: dispatch of power generating units, transmission to neighboring systems or sectors, demand side management and electricity storage [3]. Typical variations in energy systems include variations on a seasonal basis due to air temperature (e.g. between summer and winter), diurnal variations from night to day due to social factors, but also on short timescales (seconds to minutes), due to more or less random events. Large-scale integration of non-dispatchable energy sources is expected to have a strong influence on variability: solar power generation might enhance the diurnal variability, while wind power generation might induce variability on a weekly timescale. Thus, depending on the system context, the most suitable mix of flexibility varies; but thermal power plants are generally expected to have to operate with increased levels of flexibility [4–7] in order to contribute to the electricity system

* Corresponding author.
E-mail address: beiron@chalmers.se (J. Beiron).

https://doi.org/10.1016/j.apenergy.2020.115630
Received 29 April 2020; Received in revised form 28 July 2020; Accepted 29 July 2020

Nomenclature

AP	Absolute percentage deviation
β	Linear regression coefficient in surrogate models
C	Electricity system scenario with load flexibility in sector couplings
CHP	Combined heat and power; steam cycle operational mode with generation of electricity and heat.
CFQ	Steam cycle operational mode with generation of electricity and primary frequency response.
CO_2	Carbon dioxide
COND	Steam cycle operational mode with generation of electricity
CPLEX	Optimization model solver
DEA	Deaerator
DH	District heating
F	Primary frequency response delivered
FRQ	Steam cycle operational mode with generation of electricity, heat and primary frequency response.
GAMS	General Algebraic Modeling System
GT	Gas turbine
GTCC	Gas turbine combined cycle
GTCC-CHP	Gas turbine combined cycle with combined heat and power generation
HOB	Steam cycle operational mode with generation of heat only.
HRSG	Heat recovery steam generator
ISO	The International Organization for Standardization
NC	Electricity system scenario without load flexibility in sector couplings.
NG	Natural gas
P	Electricity produced
Q	District heating produced
R	Revenue
RV	Reference value
S	Steam node in optimization model
SF	Supplementary firing
SH	Superheater
ST	Steam turbine
SV	Simulated value
T	Temperature
VI	Volatility index

balancing.

Gas turbine combined cycles with combined heat and power (GTCC-CHP) production are units that deliver heat to industrial processes or district heating (DH) systems, and the operational pattern is commonly dictated by the heat demand profile. Combined cycles are well suited for flexible power generation, with possibilities for steep load gradients and quick start-up of gas turbines [8]. With the ability to operate in various modes, the bottoming steam cycle presents additional opportunities for a wide and flexible load range [9]. Thus, on a plant level, a cogeneration combined cycle can have 1) operational flexibility, as given by the minimum load level, ramp rate and cycling characteristics of the plant [10]; and 2) product flexibility, by regulating the steam flow in the steam cycle to vary the ratio of district heating, electricity and/or other products (e.g. primary frequency response) [9]. Additionally, for GTCC-CHP plants that are connected to a district heating network, thermal flexibility can also be available, e.g. by incorporating a thermal energy storage [11], or utilizing the thermal inertia of the district heating network [12]. Yet, advanced network control systems are needed to unlock flexibility in DH systems [13]. Thermal flexibility allows load shifting and decoupling of heat and electricity generation, which can be favorable in market contexts where peak electricity prices do not match peaks in heat demand [9] and support wind power integration [14]. These types of flexibility are further discussed and defined in Section 2. However, the main product for CHP plants in the Nordic region is traditionally the generation of district heating, with electricity being a byproduct sold on the energy-only market. The opportunity to deliver flexibility to the electricity system may thus be limited by the required heat production profile.

Operational flexibility is commonly studied with process modeling and given a technical perspective. The level of operational flexibility of power plants differ depending on fuel type and plant design, as reviewed by Gonzalez-Salazar et al. [8]. and operating strategies of CHP plants for efficient utilization of flexibility are reviewed in [15]. Cáceres et al. [16] modeled a combined cycle and found that supplementary firing could be of interest for peak power and load flexibility in combined cycles. Richter et al. [17] found that plant-internal steam accumulators could improve the operational flexibility of steam cycles, e.g. by lowering the minimum level of power generation. Dynamic models have been used to study the time-dependent aspects of operation and control systems in combined cycles and for evaluations of thermal stresses and lifetime costs connected to transient operation: for instance, feedforward control was found beneficial for heat recovery steam generator operation under fast load changes [18], and model predictive control strategies with stress monitoring was developed for enhanced GTCC operational flexibility [19]. Dynamic models have also been developed for computation of lifetime reduction in critical plant components during transient operation [20,21] and startup of GTCC units [22], as well as for evaluation of extra costs related to flexible operation based on predictions of residual life [23]. Additionally, Montañés et al. [24] found that integration of a post-combustion carbon capture unit did not significantly impact the GTCC load-following capability.

From a system perspective, flexibility has also been approached using optimization models, with minimization of the total system cost and simplified technology representations, to focus on economic aspects. Thermal power plant cycling costs and properties were reported to be of critical importance for cost-optimal electricity system composition [25], reduction of wind power curtailment [26] and for profitability of combined cycles [27]; allowing fast starts could be cost-optimal despite greater maintenance costs [28]. Romanchenko et al. [29] found a connection between electricity price fluctuations and cogeneration combined cycle dispatch for a district heating network, where a variable power-to-heat ratio could increase the value of CHP plants. Tools have been developed for the valuation of power plant flexibility options [10] and expected future profitability [30]. Optimization models have also been developed to study cost-efficient ways to manage energy systems with large scale wind power schemes, e.g. Mikkola and Lund [31] studied the use of existing dispatchable power plants in a CHP-dominated district heating system for more optimal system integration, that could lead to major CO_2 emission reductions.

Thus, previous studies have focused on the separate analysis of technical and economic aspects of specific flexibility measures, from energy system or power plant perspectives. However, to the best of our knowledge, a techno-economic analysis of multiple flexibility measures in heat-driven cogeneration combined cycles has insofar not been presented; that considers both CHP plant level flexibility (operational flexibility and product flexibility) and flexibility in the district heating system (thermal flexibility) together with electricity system price volatility. Furthermore, we propose a classification of CHP flexibility into three categories: operational, product and thermal flexibility; as given in Section 2. In our previous work [9], we studied the use of product flexibility in a waste-fired CHP steam cycle in combination with thermal flexibility in a district heating system. The present work expands the

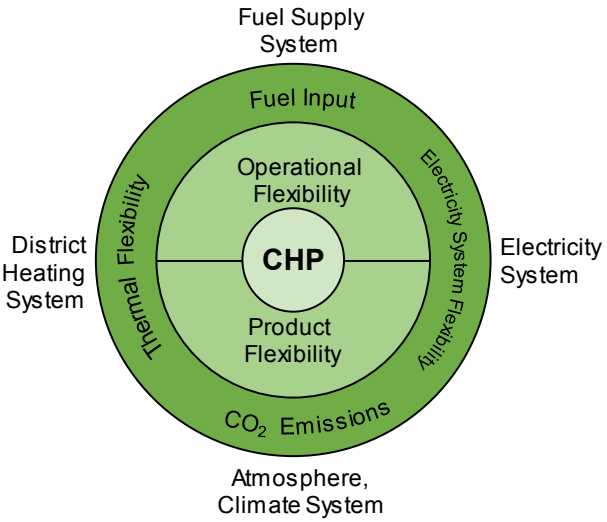

Fig. 1. Schematic of the considered types of varying boundary conditions and related flexibilities that impact the operation of a combined heat and power (CHP) plant. The light green field represents the plant level flexibilities of the CHP plant, while the outer circle contains the system level flexibilities creating the boundary conditions for the CHP plant operation. Outside of the circle are the sources of variability that trigger the need for flexibility.

analysis and evaluates the influence of plant and system level flexibility measures on the dispatch and revenue of heat-driven cogeneration combined cycles. The main novelty of the work lies in the combination of technical and economic analyses, based on dispatch optimization modeling with a detailed representation of the feasible GTCC-CHP operating region and technical plant flexibility options, coupled with price signals for future energy system scenarios that determine to what extent the flexibility options are utilized and their relative value for the plant. Additionally, we present a modeling framework with high-fidelity and surrogate process models of a reference plant, with stationary and dynamic GTCC-CHP models that are validated with reference data from steady-state and transient operation. The transient validation of a dynamic GTCC-CHP model with three parallel lines of gas turbines and heat recovery steam generators connected to one backpressure steam turbine is not present in the literature, and adds to the novelty of this work.

The starting point of the paper is a definition of the types of flexibilities considered in this work (Section 2), together with a description of the modeling framework developed (Section 3) that gives an overview of the methods used, the reference plant and the system settings. Section 4 presents the model development and validation. The results from the modeling framework are presented in Section 5 and include: the potential for flexibility in GTCC-CHP plants; the utilization of operational, product and thermal flexibility in different system contexts; and the value of flexibility measures from a plant perspective. The work is concluded in Section 6.

2. Definitions of flexibility

Different flexibility measures for the operation of heat and power generating plants and energy systems are needed to handle different types of variabilities and therefore "flexibility" has become a rather vague term. As reported in the introductory section, many works have studied flexibility from different perspectives and system levels. In this work, we propose a categorization of flexibility according to Fig. 1, that illustrates the relation between the types of flexibilities considered and the boundary conditions for variations in the heat and electricity demand, fuel supply and CO_2 emissions related to impacts on climate systems. Here, the following definitions of flexibility apply:

- **Plant level flexibilities:** technical installments that are used to vary the plant input and outputs:
  - **Operational flexibility**: the ability of a plant to vary the input thermal load from the fuel conversion system. For a GTCC-CHP plant, this corresponds to the load ranges, ramp rates and cycling properties of gas turbines and supplementary firing burners.
  - **Product flexibility**: the ability of a unit to vary the output load of a specific product by adapting product ratios (primarily the ratio between electricity and heat generation). For a steam cycle, this corresponds to using steam flow regulation in the steam cycle, e.g. a steam turbine bypass or condenser tail.
- **System level flexibilities**: the economic and system context of the plant including boundary conditions, e.g. market conditions or demand levels, that influence the plant operation and need for plant level flexibility:
  - **Thermal flexibility**: the total flexibility of the district heating system to which the plant is connected, including dispatchable generation, thermal energy storage, and demand side management; quantified as the amount of heat [MWh] that can be shifted in time.
  - **Electricity system flexibility**: the total flexibility available in the electricity system to cope with the variability of demand and generation from variable energy sources (mainly wind and solar power). This flexibility includes dispatchable generation, storage,

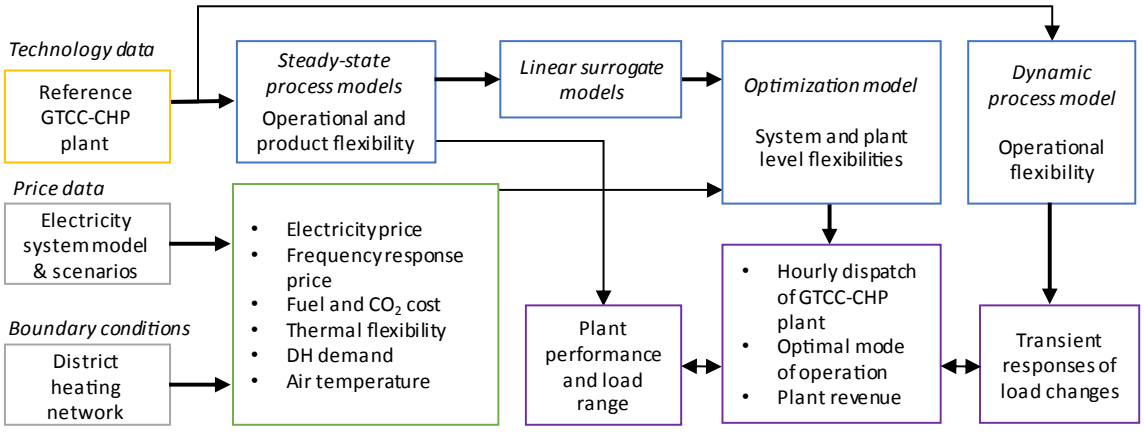

Fig. 2. Method overview. Process simulation and optimization models are linked to evaluate the synergies between plant and system level flexibilities for optimal plant operation and revenue. Blue boxes represent the models developed; purple boxes indicate model outputs. The yellow box is the reference plant, from which technology data is obtained. System boundary conditions and price data are indicated by grey boxes, which give input to the optimization model (green box).

Table 1
Input parameters for electricity price scenarios of relevance to the optimization model analyses. NG is natural gas. C/NC refer to scenarios with/without flexibility in sector coupled loads, see Section 3.3.

Electricity price scenario		2016	2030C/NC	2040C/NC	2050C/NC
Fuel cost [€/MWh$_{fuel}$]	*Low*	20 (NG)	15 (NG)	15 (NG)	50 (biogas)
	Base	30 (NG)	30 (NG)	25 (NG)	77 (biogas)
	High	40 (NG)	45 (NG)	45 (NG)	100 (biogas)
CO_2 cost [€/ton$_{CO2}$] or [€/MWh$_{fuel}$]		5.54 1.17 (NG)	40 8.43 (NG)	100 21.06 (NG)	400 0 (biogas)
Thermal flexibility [MWh$_{heat}$]		0–100 000			
Product flexibility		Yes/No			

transmission, sector coupling and demand side management; and is quantified by the electricity price profile, or price volatility, for the given system.
- **Fuel supply system:** the supply and demand of a fuel that influences the fuel cost.
- **Climate system:** the impact of environmental aspects on plant operation, for example costs for emitting CO_2, that adds to the plant operational expenditures and might incentivize flexibility in operation that improves efficiency in fuel use, or fuel substitution.

3. Method

The flexibility types in Fig. 1 come from different regimes and levels of the energy system and are commonly handled separately. This work is based on a modeling framework that combines process simulation and dispatch optimization models of a GTCC-CHP plant. System and plant level models are soft-linked to provide a wide perspective on the utilization of GTCC-CHP flexibility in energy systems. Fig. 2 gives an overview of the method and the relation between the models. A similar multi-model approach has previously been used by, for example, MacDowell and Staffell [32].

Four types of models of a GTCC-CHP plant are developed: steady-state process simulation models and surrogate models, a dynamic process simulation model and a plant dispatch optimization model. The process simulation models are developed based on a reference GTCC-CHP plant and validated with steady-state and transient operational data. The steady-state process simulation models give the static performance and load range of the plant, considering the operational modes and load levels available with operational and product flexibility. The dynamic process model simulates the transients of GTCC-CHP load changes. The plant performance results and feasible operating region are linked to the optimization model by the derivation of linear surrogate models that act as constraints in the optimization model. The optimization model evaluates the impact on GTCC-CHP plant operation and revenue of:

- Product flexibility of the steam cycle, Section 3.2.
- District heating system thermal flexibility.
- Electricity price volatility, Section 3.3.
- Fuel and/or CO_2 cost.

Table 1 gives the evaluated magnitudes of the flexibilities implemented. System level flexibility inputs are given as boundary conditions for the level of thermal flexibility in the district heating (DH) system, fuel and CO_2 costs and an electricity price profile. The electricity price profiles are obtained from an energy system model [33] that finds the cost-optimal electricity system generation technology mix for a given system and scenario. The fuel cost levels include variations in both fuel cost and CO_2 cost, since the CO_2 cost paid by the plant is directly related to the carbon content in the fuel used. Currently, Swedish CHP plants pay the European Union emissions trading system carbon cost and are exempt from additional national carbon taxation. The CO_2 costs and base level fuel costs are obtained from [33] for the 2030–2050 scenarios. For 2016, the natural gas price is set to 30 €/MWh$_{fuel}$ [34] and the CO_2 price to 5.54 €/ton CO_2 (average value for 2016) [35]. In the 2050 scenarios, natural gas is substituted by biogas as the natural gas plus CO_2 costs exceed the cost of biogas.

The main results obtained from the modeling framework include: 1) static and dynamic perspectives on the technical *potential* for flexibility in GTCC-CHP plants, considering operational and product flexibility; 2) the optimal *utilization* of flexibility measures (operational, product, thermal) as a function of system setting; and 3) the economic *value* of flexibility measures, for the GTCC-CHP plant, as expressed by the impact

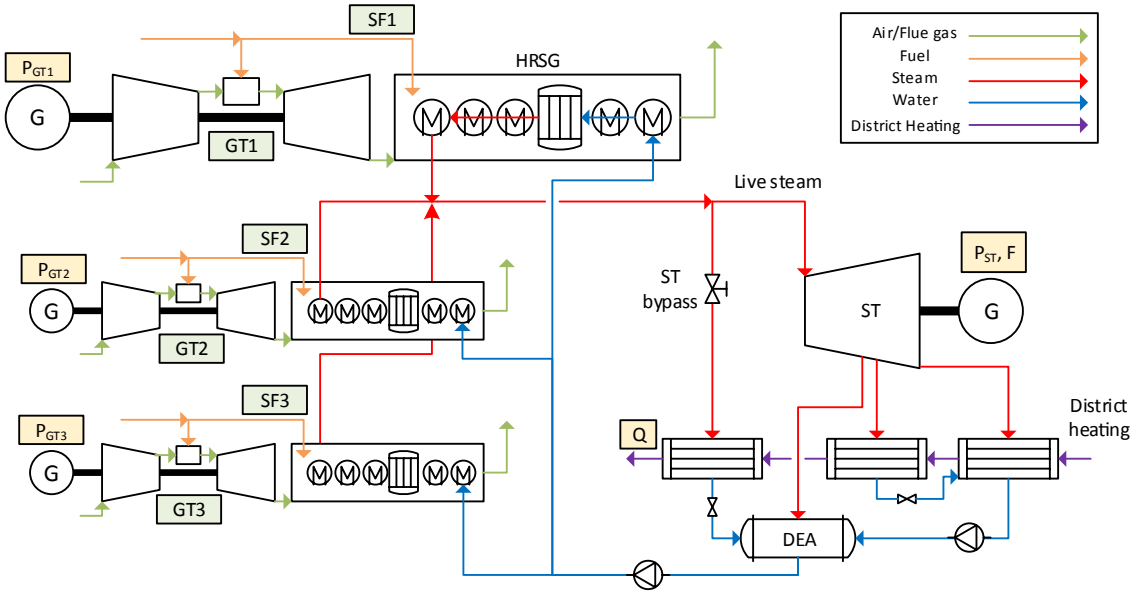

Fig. 3. Simplified process schematic of the reference plant. DEA = deaerator, GT = gas turbine, HRSG = heat recovery steam generator, SF = supplementary firing, ST = steam turbine. Letters in green boxes refer to fuel input points (cf. Fig. 6). Letters in yellow boxes refer to feasible products: P = electricity, Q = district heating, F = primary frequency response.

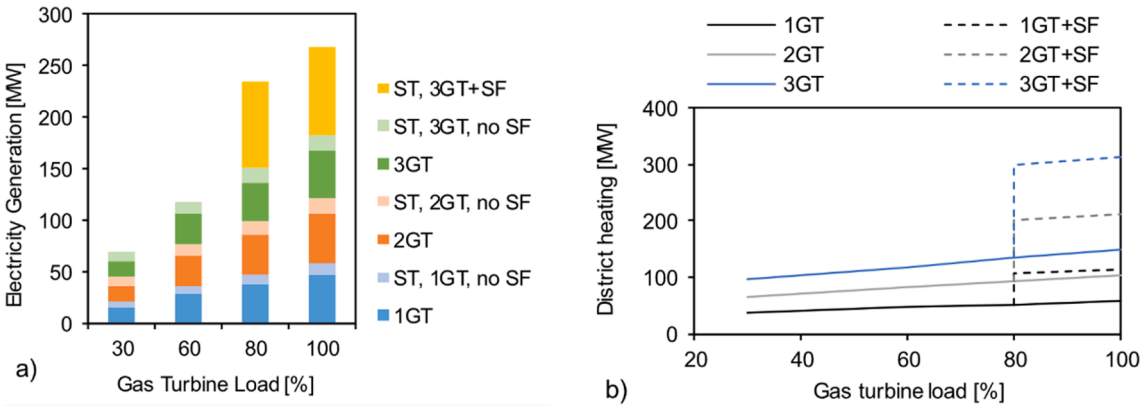

Fig. 4. The (a) electric and (b) district heating load ranges of the reference plant, as a function of gas turbine (GT) and supplementary firing (SF) loads. (a) Incremental electricity generation for gas and steam turbines, e.g. the bar height of "ST, 2GT, no SF" is the increase in steam turbine (ST) output when the second (2GT) is started. (b) Heat output for operation with one (1GT, black line), two (2GT, grey), and three (3GT, blue) gas turbines as a function of gas turbine load. The yellow bars in (a) and the dashed lines (GT + SF) in (b) mark operation with the maximum load of supplementary firing.

on plant revenue. Furthermore, the models span a wide range of timeframes: the dynamic model simulates minute-to-hour ramp times with a short (second or sub-second) time resolution, while the optimization model works on an hourly timescale over the course of a CHP plant's heating season, summing to annual values.

3.1. Reference plant

The reference plant in this study is a combined heat and power gas turbine combined cycle plant with a nominal capacity of 300 MW heat and 250 MW electricity, including three gas turbines with nominal power 43 MW (ISO conditions). The plant is operated as a mid/peak load plant in the district heating system of Gothenburg, Sweden. Fig. 3 shows a simplified schematic of the plant, that consists of three parallel lines with one gas turbine (GT), single-pressure heat recovery steam generator (HRSG) and supplementary firing (SF) burner each; and one steam turbine (ST). Both the gas turbines and the supplementary firing use natural gas as a fuel. Live steam conditions at full load with supplementary firing are 540 °C and 95 bar. District heating is extracted from the steam cycle condensers via one backpressure and one extraction condenser. There is also a steam turbine bypass possibility, where the live steam can be condensed in a third condenser, producing district heating or being cooled by river water. Additional reference plant information can be found in Ref [36].

The combined cycle can be operated in several load points for cogeneration of heat and electricity, by varying the gas turbine (GT) and supplementary firing (SF) loads. Fig. 4 shows a) the electric and b) the district heating load range of the reference plant. Supplementary firing can be used for gas turbine loads of 80% or more, yielding an increased generation of heat and electricity from the steam turbine. Without supplementary firing, the gas turbines' contribution to the electricity generation is larger than that of the steam turbine. With supplementary firing, the electricity production of the three gas turbines is comparable to the steam turbine electricity generation. Thus, the three parallel lines and the possibility to use supplementary firing gives the CHP plant a high potential for flexibility in operation.

3.2. Product flexibility of the steam cycle

The operating region of the GTCC-CHP plant is expanded with steam cycle operational modes, i.e. by increasing the plant product flexibility. In this work, five steam cycle modes, previously proposed in [9], of different product ratios are modeled:

- CHP mode: conventional operation, producing heat and electricity with a fixed power-to-heat ratio.
- HOB mode: operation with full bypass of the steam turbine, only producing heat from the steam cycle. Gas turbines still generate electricity.
- FRQ mode: operation that generates heat and electricity, together with delivery of primary frequency response. The maximum amount of frequency response for a given steam turbine load level is delivered. Gas turbines do not deliver frequency response.
- COND mode: condensing operation, only producing electricity.
- CFQ mode: condensing operation with delivery of primary frequency response.

Combinations of modes could be feasible in practice, but are not considered in the optimization model, e.g. only 100% steam turbine bypass operation is modeled and no partial bypass options. In Sweden, the focus region in this work, primary frequency response (denoted FCR-N in the Swedish market) is a symmetrical product that is traded on an hourly market, i.e. the same timescale as the electricity spot market. Even though frequency regulation is required on short timescales, it is in the optimization model considered a product with an hourly timeframe. Although gas turbines might have a potential to deliver frequency response services as well, in this work we limit the analysis to the operational flexibility of gas turbines. The condensing operating modes are with the current legislation not allowed, i.e. CHP plants cannot produce electricity if there is not sufficient demand for heat to motivate operation. However, in future electricity system scenarios, there might be times with shortage of electricity supply that might incentivize a shift in policy, allowing CHP plants to generate electricity using condensing operation when the heat demand is low. It is assumed that an unlimited supply of cooling water is accessible for such purposes.

3.3. Electricity system model, scenarios and price volatility

The electricity price input profiles are results from the energy system scenarios modeled in [33], where the "Hours-to-Decades" model gives the electricity system generation, transmission and storage capacity for future scenarios with and without sectorial collaboration. In the scenarios, the cost of emitting CO_2 is successively increased from 40 €/ton in 2030 to 400 €/ton in 2050 [33]. Sectorial collaboration (denoted "C") here refers to sector coupling and flexibility in terms of load shifting of electric loads within the transport [37], industrial [38] and heat sectors. In scenarios without sectorial collaboration (denoted "NC"), the sector coupling is still present, but the loads are fixed, predetermined and not flexible in time. The geographical price region corresponds to the South

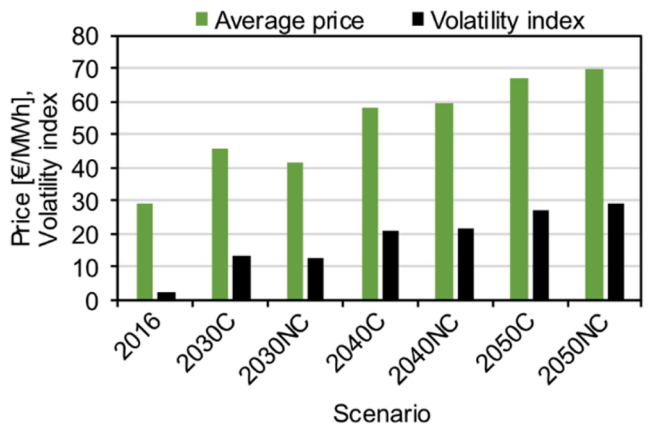

Fig. 5. Average electricity price and volatility index for the electricity price scenarios, during the plant operating period. Scenarios with and without flexible sectorial coupling are denoted with "C" and "NC", respectively.

Table 2
Ramp time and ramp rate for the three cases simulated, corresponding to load changes between full and zero load for supplementary firing (SF), and full and minimum load for gas turbines (GT). Based on reference plant data.

Ramp case	SF ramp time [min]	SF ramp rate [%/min]	GT ramp time [min]	GT ramp rate [%/min]
Slow	120	0.8	60	1.2
Mid	60	1.7	30	2.3
Fast	30	3.3	15	4.7

of Sweden. The electricity price profiles are available in [9].

Input profiles for hourly electricity and frequency response prices are also obtained for the reference Year 2016 [39,40]. The primary frequency response price profile of 2016 is used as input in all scenarios, independent of the year.

A volatility index, *VI*, defined as:

$$VI = \frac{\int_{t_1}^{t_2} (price(t) - average\ \ price)^2 dt}{t_2 - t_1} \cdot \frac{1}{100} \quad (1)$$

is used to quantify the price volatility of the electricity price in the studied scenarios [9]. Fig. 5 compares the average electricity price and volatility index for the seven scenario price profiles, during the plant's operating period. The average price and volatility index increase over time from 2016 to the 2050 profiles, ranging from 29 to 69 €/MWh and 2.4 to 29.1, respectively.

3.4. Dynamic aspects of operational flexibility

Energy system optimization models often assume that power plants are ideal static plants that can change from one operational point to another instantaneously, while in practice power plant load changes are associated with a ramp time. The impact of this assumption on the economic results, and the value of fast ramp rates, are evaluated by dynamic simulation of gas turbine and supplementary firing load changes with different ramp times. For supplementary firing, the load change considered is between full and zero load. For gas turbines, the load change is between full and minimum load (100% and 30% of rated power). Three ramp cases are compared, denoted "slow", "mid" and "fast", and the ramps are assumed to be linear, with a constant ramp rate. Table 2 gives the ramp times and ramp rates of each case. The "slow" ramp case is based on reference plant data for transient operation that is adapted to the relatively slow dynamics of the district heating system, whereas the ramp rates in the "mid" and "fast" cases have been increased with a factor 2 and 4, respectively. The ramp cases are simulated with the dynamic model (Section 4.2.3). The resulting response signals for the electricity output from the steam turbine and gas turbines are summed and integrated to find the transient electricity generation between time t_1 and t_2, similar to the work by Montañés et al. [41]:

$$P = \int_{t_1}^{t_2} P(t)dt \quad (2)$$

Based on the transient electricity generation during ramp events, the revenue from electricity generation is calculated as:

$$R = \int_{t_1}^{t_2} C_{el}(t)P(t)dt \quad (3)$$

The revenue difference between static (instantaneous load change) and dynamic operation (load change with ramp rate) is then:

$$\Delta R = \left| R_{static} - R_{ramp} \right| \quad (4)$$

4. Modeling

4.1. Optimization model

The optimization model used in this work is based on our previous work [9]. The model is developed using the high-level modeling language GAMS. Below is a brief description of the model relevant to the present investigation. The model formulation is described in detail in Appendix A.

The mixed integer linear programming model optimizes the

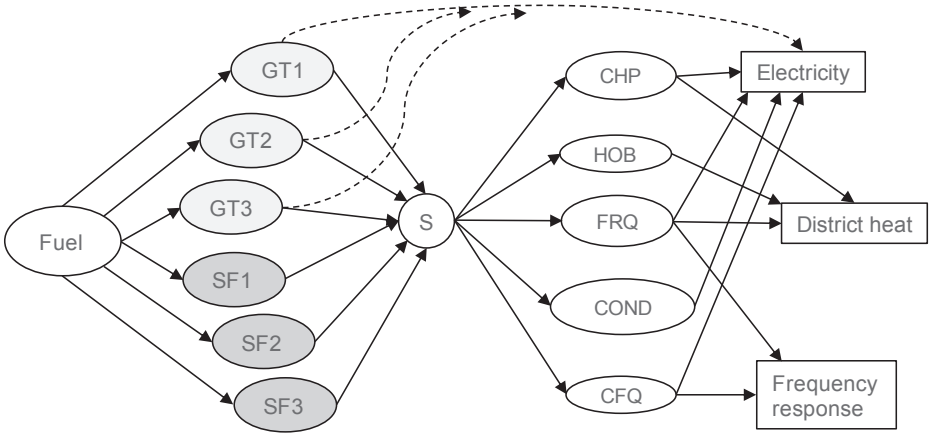

Fig. 6. Overview of the optimization model network framework, emphasizing the opportunities for flexible operation, including gas turbine (GT) and supplementary firing (SF) fuel use and the operational modes of the steam cycle (CHP, HOB, FRQ, COND, CFQ) that enable product flexibility.

operation of the CHP plant, with respect to income from electricity and primary frequency response delivery, start-up cost and fuel and CO_2 costs. The objective of the model is to maximize the plant revenue, while satisfying a given hourly heat demand. However, heat production might be decoupled from the demand and load shifted depending on the DH system thermal flexibility. There is, thus, no income associated with heat sales in the objective function, even though heat sales will, of course, generate revenue in practice. The decision variables that the model optimizes are: the gas turbine loads, supplementary firing loads and selection of the steam cycle operational mode.

Fig. 6 presents the network flow model structure applied to describe the energy flows and production in the GTCC-CHP plant. Fuel (natural gas or biogas) is fed to gas turbines and supplementary firing burners, which generate steam via the heat recovery steam generator, represented by the node *S*. The live steam is then allocated to one of the five steam cycle modes (CHP, HOB, FRQ, COND, CFQ), resulting in generation of electricity, district heat and/or frequency response delivery. The plant production for different modes and loads is given by linear surrogate models derived from process models based on the reference CHP plant, as described in Section 4.2.2. Only one mode can be active at a time. Constraints for gas turbine and supplementary firing dispatch are included to ensure feasible operating patterns. Load changes are assumed to happen instantaneously; this assumption is evaluated using dynamic simulation (Sections 3.3 and 5.3.2).

The modeling time period considered is the heat-generation season for Year 2016 with hourly resolution (3663 h). The input profile for district heating demand consists of hourly measurements from the reference plant, where the heat demand is assumed to equal the measured plant heat production. The 2016 heat demand profile is used in all analyses and plotted in Fig. 14. The thermal flexibility is modeled as a thermal energy storage with an energy balance equation. Price data are inputs to the model, according to Section 3 and Table 1. Thus, the model has perfect foresight. The model is solved using the CPLEX solver, with a relative optimality criterion of 0.05.

4.2. Process simulation models

4.2.1. Stationary process models

Stationary process models of the reference plant are developed in the steady-state modeling environment EBSILON Professional [42]. One model each is developed for the five steam cycle modes. Fig. 3 provides an overview of the models, that are based on the following components: On the flue gas side, there are three parallel lines with gas turbines (GT1-3), supplementary firing duct burners (SF1-3) and a HRSG represented by a flue gas train with gas-two-phase heat exchangers (economizer, evaporator, drum and three superheaters) where the steam is generated. On the steam side, there is a steam turbine (ST) with two extractions for the deaerator (DEA) and extraction condenser, a backpressure condenser, feed water pumps and steam attemperators. Each component is modeled with mass and energy balances that must be satisfied by the computed solution. The gas turbines are modeled based on characteristic curves provided by the manufacturer, with specified performance data depending on the ambient temperature and load level. The steam turbine model is based on Stodola's law [43] and accounts for part load performance. The modeling practice is further outlined in Ref. [44].

The listed components refer to the CHP mode and is based on the reference plant configuration. The following model features distinguishe the five modes from each other: A steam turbine bypass is added to the HOB, FRQ and CFQ process models. The bypassed steam is condensed in an additional steam condenser, that is cooled by district heating water in the HOB and FRQ modes, or cooling water in the CFQ mode. In the HOB mode, 100% of the live steam flow is bypassed so that no electricity is generated by the steam turbine. In the FRQ and CFQ modes, the ratio of bypassed live steam is between 23 and 45% of the total steam flow, so that the maximum amount of frequency response possible is delivered at all load levels. The COND mode only uses the backpressure condenser which is cooled by cooling water instead of district heating water.

The models simulate the steam cycle performance in design and off-design operation for the five modes, for specified gas turbine and supplementary firing loads. Input specifications are also given for district heating return temperature and mass flow, or cooling water inlet and outlet temperatures (assumed to be 10 and 15 °C, respectively). The calculated results include the electricity and district heating generation. The CHP mode model is validated with steady-state reference data for three load cases, Section 4.3.1.

4.2.2. Surrogate process models

The stationary process models are linearized to surrogate models that describe the process performance; i.e. how the electricity, DH, and frequency response delivery depend on the plant operation. Resulting equations on the form given in Eq. (5) and (6) are included in the optimization model to represent the plant performance. Eq. (5) gives the gas turbine fuel consumption (*Fuel*) and electricity generation (P_{GT}) as a function of gas turbine load and air temperature. Eq. (6) gives the steam cycle electricity (P_{ST}), district heating (Q) and frequency response delivery (F) as functions of gas turbine load and supplementary firing load. The coefficients, β, are obtained from linear regression analysis of simulation results from the stationary process models and are specific to each response variable. The coefficients in Eq. (6) are also specified for each steam cycle mode (CHP, HOB, FRQ, COND, CFQ). The products (P_{ST}, Q, F) are marked in Fig. 3. The CHP mode surrogate model is validated with steady-state data, shown in Section 4.3.1.

$$Fuel, P_{GT}(t, GT) = Load(t, GT)\beta_{Load} + T_{air}(t)\beta_{Temp} + \beta_0 \tag{5}$$

$$\begin{aligned} P_{ST}, Q, F(t) =& \beta_{GT}\sum_{GT}\left(Load(t, GT)\beta_{GTLoad} + \beta_{0,GTLoad}\right) + \beta_{0,GT} \\ &+ \beta_{SF}\sum_{SF} Load(t, SF) + \beta_{0,SF} \end{aligned} \tag{6}$$

4.2.3. Dynamic process model

A dynamic process model based on the reference plant is developed in the modeling language Modelica [45], using the software Dymola [46] and the Thermal Power component library [47]. The component library has been used in several studies, for example [24,48–50]. The model is based on physical equations, algebraic and differential, including mass and energy balances for the system components. The model is developed using modeling practices that are outlined in previous work by the authors, that present dynamic models of steam cycles [48] and combined cycles [18,24,51]. Here, we only give a brief overview of the model features that are specific to this work and instead focus on the model validation and linking with the optimization model for economic evaluation of ramp rates, as these are the parts of the method and modeling procedure of novelty in this study. For a thorough description of the dynamic modeling method, the interested reader is referred to the cited works.

The dynamic model includes the process parts illustrated in Fig. 3. The heat recovery steam generators (HRSG) and steam cycle include a series of gas-two-phase heat exchangers (economizer, evaporator and superheaters), a steam drum, feed water pumps, condensers and a steam turbine component accounting for part load efficiency based on Stodola's law. The supplementary firing is modeled as a duct with a heat source connected to it, where the combustion of fuel is assumed to be fast. The gas turbines are modeled as algebraic components as described in Section 4.2.1, where the exhaust gas mass flow and temperature and electricity generation are functions of load and inlet air temperature. Dynamically, a static gas turbine component is motivated by the relatively short timescale of the gas turbines compared to the HRSG [52].

The input values to the model are: ambient air temperature, gas turbine and supplementary firing loads, district heating return temperature and mass flow, and set point temperatures for steam attemperators. Outputs are computed for response variables, such as electricity

Table 3
Validation results for the three process models, expressed as absolute percentage deviation for selected process variables. SH = superheater, DH = district heating. Dashes indicate that the value is a model input (steady-state model), or not a calculated output (surrogate model).

	Absolute percentage deviation [%]								
Model	Steady-state model			Linear surrogate model			Dynamic model		
Load case	1	2	3	1	2	3	1	2	3
Drum pressure	–	–	–	–	–	–	0.1	0.7	0.5
SH1 outlet temperature	1.2	4.6	3.6	–	–	–	0.6	2.4	0.6
SH2 outlet temperature	1.3	3.6	2.5	–	–	–	0.9	2.3	0.7
Live steam temperature	1.6	3.0	2.2	–	–	–	2.1	0.6	1.0
Total live steam flow	0.1	1.3	6.7	–	–	–	5.4	3.5	0.4
DH supply temperature	–	–	–	–	–	–	2.5	4.7	3.7
Steam turbine electricity generation	0.1	13.2	4.5	0.1	15.3	6.4	2.5	25.9	35.0
DH generation	1.1	6.8	7.2	3.2	11.2	9.8	3.2	1.8	4.9
	Deviation [MW]								
Steam turbine electricity generation	−0.1	2.8	0.6	0.0	3.3	0.9	−3.1	5.6	5
DH generation	3.3	−7.6	−5.5	9.6	−12.5	−7.5	−9.7	2	3.8

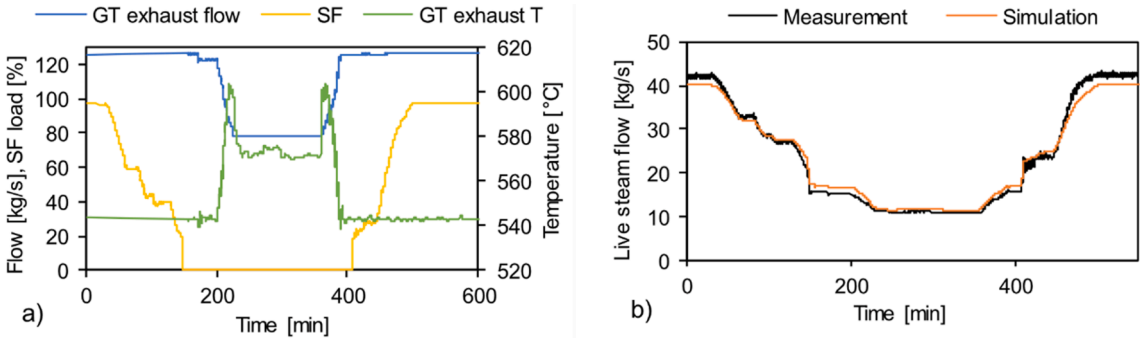

Fig. 7. (a) Input profiles for the dynamic model transient validation, showing gas turbine (GT) exhaust flow (blue) and temperature (green), and supplementary firing (SF) load (yellow). (b) Transient validation simulation response (orange) and reference measurements (black) for the live steam flow from one HRSG.

and heat generation, and pressure, temperature and flow at several points in the steam cycle and HRSG. The model is solved using the Dassl integration algorithm, with a sufficient number of intervals to satisfy a tolerance level of 0.0001, resulting in a second or sub-second time resolution. The dynamic model is validated with steady-state and transient data from the reference plant, see Section 4.3.

4.3. Validation of process simulation models

4.3.1. Validation of process models with steady-state data from the reference plant

The stationary, surrogate and dynamic process simulation models are validated with steady-state data from the reference plant for: 1) Full load operation of all gas turbines and supplementary firing. 2) Full load operation of two gas turbines, no supplementary firing. 3) Part load operation of two gas turbines (approx. 35% of full load), no supplementary firing. For each load level, the district heating mass flow and supply and return temperatures are specified inputs, and the steam turbine electricity generation and steam parameters are calculated outputs. For each model and load case, the simulated value (SV) is compared to the reference value (RV) by calculation of the absolute percentage deviation (AP):

$$AP = \frac{|SV - RV|}{RV} \cdot 100 \tag{7}$$

The percentage deviations for each load case are presented in Table 3 for the three model types, together with the deviation between SV and RV for the main response variables: steam turbine electricity generation and district heating generation. The simulated values show good agreement with the reference data, with deviations of less than 5% for most process variables and load cases. The simulated steam turbine electricity generation and district heating output deviates from the reference to a greater extent (up to 35%) for load cases 2 and 3 (part load operation). However, given the large load range of the steam turbine, from approximately 10% to 100% of rated power, deviations at low loads were expected as the steam turbine efficiency varies over such large load ranges. Furthermore, the deviations at lower load levels are comparable to those of full load (load case 1), even though the part load percentage deviations are large.

4.3.2. Validation of dynamic process model with transient data from the reference plant

The dynamic process model is validated with transient operational data from the reference plant. Plant measurements are from ten hours of “normal” plant operation, i.e. suited for district heating network dynamics, and include gas turbine and supplementary firing load changes. Fig. 7a presents the gas turbine exhaust mass flow and temperature, and supplementary firing load used as inputs to the dynamic model for the transient validation. The simulated responses for live steam flow, drum pressure and superheater outlet temperatures are compared to the measurements. For example, Fig. 7b plots the measured and simulated response for live steam flow from one HRSG while the remaining variables are compared in Appendix B. The simulated response shows good agreement with the transient data for the measured flow, although a steady-state error (quantified in Section 4.3.1) is present as a discrepancy between the two curves. For the purpose of this study, with emphasis on the economic value of increased ramp rate, the model is considered an adequate representation of the reference GTCC-CHP

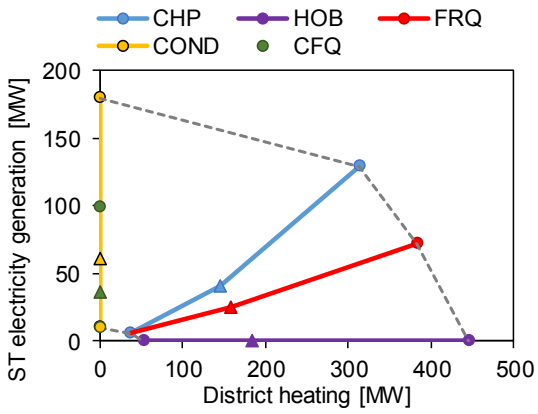

Fig. 8. Steam cycle load range expansion with the five operational modes: blue = CHP, purple = HOB, red = FRQ, yellow = COND, green dots = CFQ. The x-axis gives the district heating output, and the y-axis indicates the corresponding steam turbine (ST) electricity generation. Triangles mark the simulated plant output at full gas turbine load (3GT) without supplementary firing, for each mode.

plant.

5. Results and discussion

The results are presented in three parts. The first part covers the steam cycle load range expansion from product flexibility and is based on results from the stationary process modeling of the five steam cycle operational modes, introduced in Section 3.2. The second part presents results from the optimization model, focusing on the utilization of the static plant level flexibilities; i.e. trends relating to the load levels of gas turbines and supplementary firing and the dispatch of steam cycle operational modes; in system settings with varying degrees of thermal flexibility and electricity price volatility. Additionally, the value of product and thermal flexibility is estimated. The third part concerns the dynamic plant operation and presents results from ramp rate simulations, related to operational flexibility, that complements the static analyses in Sections 5.1 and 5.2. Optimization model results (e.g. the number of ramp events occurring during one year) are combined with the dynamic modeling results to estimate the value of operational flexibility.

5.1. Product flexibility and load range expansion

Fig. 8 illustrates the steam cycle load range expansion obtained from product flexibility, based on the process simulations. The CHP mode, as given by the blue line, represents current operation of the reference plant steam cycle. The area enclosed by the dashed lines and the yellow (COND/CFQ) and purple (HOB) lines represents the increased number of possible operational points with product flexibility. The steam turbine electricity generation may, thus, be increased by 49% without supplementary firing, and 39% with supplementary firing, compared to conventional CHP operation. The corresponding numbers for district heating generation are 27% and 42% increase, respectively. The minimum generation levels of either heat or steam turbine electricity may be decreased down to 0 MW with product flexibility.

5.2. Plant utilization and revenue with product and thermal flexibility

The following five sections present results relating to the influence of product flexibility, thermal flexibility, electricity price volatility and fuel/carbon cost on the annual plant revenue and the optimal utilization of steam cycle modes, gas turbines and supplementary firing.

5.2.1. Impact on plant revenue

Fig. 9 shows the impact on plant revenue from flexibility for four electricity price scenarios. Fig. 9a plots the increase in annual plant revenue from optimal operation in conventional CHP mode when implementing thermal flexibility, i.e. relative to the revenue without thermal flexibility. Fig. 9b plots the increase in revenue from optimal operation when implementing product flexibility, i.e. relative to a conventional CHP mode with the same level of thermal flexibility. The total revenue increase from operation with both thermal and product flexibility is, thus, the sum of Fig. 9a and b.

Both types of flexibility increase revenue, although not in synergy. For operation without product flexibility, the revenue increase grows with thermal flexibility, up to 14 M€ (Fig. 9a). If product flexibility is added, the additional revenue increase is larger at low levels of thermal flexibility, up to 9 M€ (Fig. 9b). As a reference, 1 000 MWh heat corresponds to the order of magnitude of hot water accumulation tanks. Thus, product flexibility is the most valuable in district heating systems with limited thermal flexibility (<1 000 MWh), while thermal flexibility becomes beneficial at larger levels of thermal flexibility (>1 000 MWh), e.g. by implementing a seasonal heat storage. The sum of revenue increase from both product and thermal flexibility is between 2.5 and 16.5 M€ depending on the scenario and level of thermal flexibility. If assuming a district heating price of 35 €/MWh, a 2.5 M€ increase in revenue could in the 2016 case correspond to a 58% increase in the total plant revenue.

The increase in revenue from product flexibility is explained by operation in HOB mode (Section 5.2.2) that reduces fuel costs; and the plant versatility is used to match outputs to market volatility and gives the plant resilience to price fluctuations. Similar findings have been presented for waste-to-energy plants [9]. Another benefit of product flexibility is that it should be a low-cost measure to implement for the plant, as the process components are usually already installed, and only

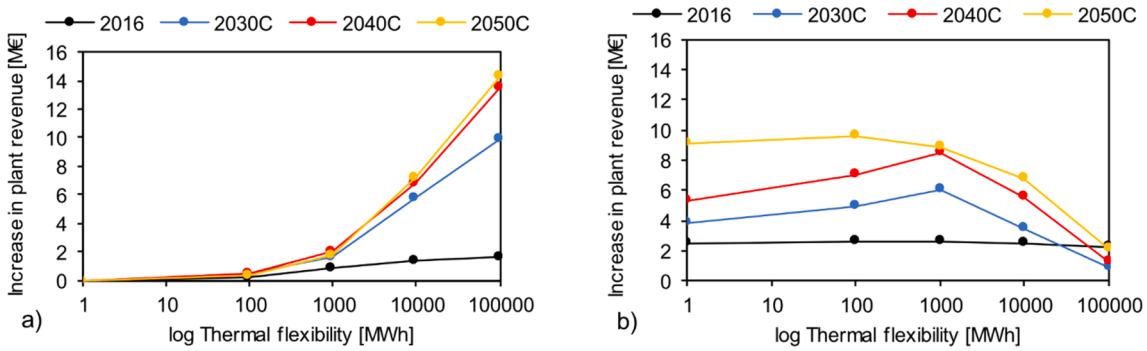

Fig. 9. (a) Increase in plant annual revenue from optimal operation with thermal flexibility and no product flexibility; (b) additional increase in revenue from operation with product flexibility, for four electricity price scenarios. The total revenue increase from operation with product and thermal flexibilities is the sum of (a) and (b). NC-scenarios are omitted but follow similar trends as the C-scenarios for the corresponding year. Note the logarithmic scale on the x-axes.

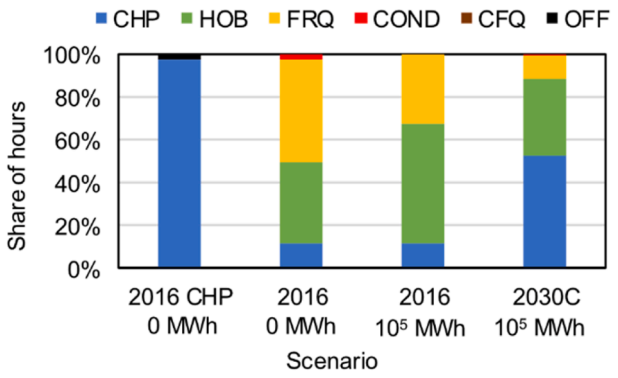

Fig. 10. Optimal steam cycle operational mode distributions and utilization of product flexibility for the 2016 data and the 2030C scenario. CHP = operation without product flexibility. The thermal flexibility is given in MWh.

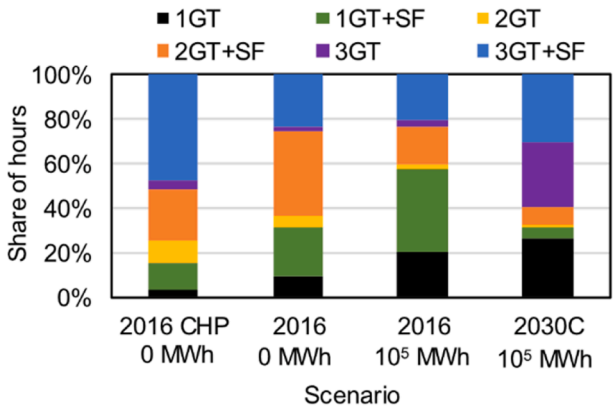

Fig. 11. Optimal utilization of gas turbine and supplementary firing operational modes for 2016 and 2030C. CHP = operation without product flexibility. The thermal flexibility available is given in MWh.

modifications of the control system could be necessary.

Thermal flexibility increases the revenue by enabling operation that follows the electricity price profile rather than the heat demand profile (Section 5.3.1). However, this work quantifies the impact on revenue from a plant perspective. If a system perspective is applied, the value of thermal flexibility could be even higher, given that thermal flexibility might be used also by and impact the dispatch of other production units, e.g. for peak shaving to avoid the use of units that are associated with high operational expenditures and/or CO_2 emissions.

The increase in revenue is larger for scenarios with high electricity price volatility indices (cf. 2016 (VI = 2.4) and 2040C (VI = 20.8)); in which the high-price and low-price periods promotes thermal load shifting, and the average electricity price increases (Fig. 5). Thus, for current market contexts with low price volatility, the profitability of flexibility measures seems limited; policy measures that incentivize additional installations of, e.g., wind power must be introduced for CHP plant flexibility to increase in value.

5.2.2. *Utilization of product flexibility*

Section 5.2.1 indicates that product flexibility may increase the revenue of a GTCC-CHP plant. This section presents results on which of the operational modes that are utilized and the type of benefits that they provide. Fig. 10 shows the optimal distribution of operational hours between steam cycle modes for 2016 (historical data) and the 2030C scenario, with a specified thermal flexibility of either 0 or 100 000 MWh. The mode distributions in the 2040 and 2050 scenarios are similar to the shown 2030C scenario, and are presented in Appendix C.

Without product and thermal flexibility (2016 CHP), the steam cycle dispatch will, of course, only consist of CHP mode. As product and thermal flexibilities are added, the distribution of hours between modes shifts. With product flexibility, a significant share of hours is allocated to the HOB (30% in 2016) and FRQ modes (50% in 2016). Compared to the CHP mode, HOB-operation yields increased heat generation (Fig. 8) for the same level of fuel input. Thus, a heat demand that would require full load operation in CHP mode, can be provided by operating at part load in HOB mode, with reduced fuel consumption and operational expenditures. As a consequence, the plant utilization decreases with 10%. The HOB mode is, thus, incentivized by high fuel and CO_2 costs compared to the electricity price. The FRQ mode might be favorable when the frequency response price is higher than the electricity price but competes with the HOB mode that is also dispatched when electricity prices are low. Condensing modes are used sparingly, <5%, since the main objective of the plant operation is heat generation, and increased plant utilization is limited by unfavorable market conditions.

With the addition of thermal flexibility, the ratio between HOB/FRQ mode shifts; in 2016, the opportunity to shift heat production in time increases the share of HOB operation to 50%. However, with the increased electricity price volatility in the 2030C scenario, CHP operation increases instead of HOB (50% CHP in 2030C vs. 10% in 2016), due to a larger number of hours with high electricity price (Fig. 5) that makes combined electricity and heat generation profitable. The mode distribution is not significantly impacted by the level of thermal flexibility (cf. 2016 0 MWh and 2016 10^5 MWh). Thermal flexibility may, thus, reduce the utilization of operational modes, although the HOB mode is still advantageous to reduce the operational costs of the combined cycle.

5.2.3. *Gas turbine and supplementary firing utilization*

The operation of gas turbines and supplementary firing is influenced by the implementation of product and thermal flexibility. Fig. 11 presents the optimal gas turbine and supplementary firing dispatch, in terms of number of hours that the plant is operated using one, two, or three gas turbines (GT) with/without supplementary firing (SF) for 2016 data and the 2030C scenario. Similar to Fig. 10, the two leftmost bars are without product and/or thermal flexibility. The distributions of the 2040–2050 scenarios are similar to the 2030C scenario and are shown in Appendix C.

Without flexibility measures, the distribution of hours is dictated by load-following operation based on the heat demand profile, and the operational hours are spread over 1GT, 2GT and 3GT operation, with SF. In 2016 CHP, 50% of hours involve operation of all three gas turbines with supplementary firing. As product flexibility is added, the share of 3GT + SF is reduced to 25% in combination with HOB operation of the steam cycle, as discussed in Section 5.2.2, and fewer gas turbines are dispatched for production to reduce fuel expenditures. In 2016, this trend is enhanced with the implementation of thermal flexibility, that further reduces the utilization of gas turbines and fuel costs: 55% of operational hours involve operation with only one gas turbine, often in combination with supplementary firing (around 40% 1GT + SF). Around 20% of operational hours are still allocated to high-load 3GT + SF operation, indicating that there are still a certain share of hours when electricity prices are high enough to motivate full load operation with gas turbines.

With the increased electricity price volatility and average price of 2030C, the number of hours with profitable electricity prices increases, so that the share of operational hours with all three gas turbines active reach 60%. The gas turbine operational hours then concentrate around low-load (1GT) or high-load operation (3GT or 3GT + SF) in a bimodal fashion, depending on the electricity price. Thus, the use of gas turbines is influenced by the electricity price, and supplementary firing is dispatched to 1) maximize the steam turbine electricity generation when electricity prices are favorable; 2) maximize the steam cycle heat generation, coupled with HOB operation (Fig. 10), when electricity prices are low and gas turbine operation is not profitable.

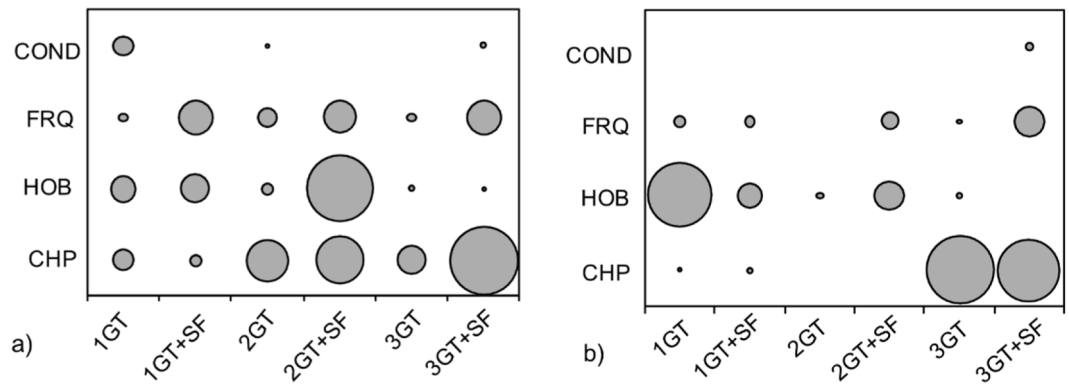

Fig. 12. Bubble charts showing the utilization of operational points in the 2030C scenario (a) without thermal flexibility and (b) with thermal flexibility. The x-axis refers to the operation of gas turbines (GT) and supplementary firing (SF), while the y-axis gives the steam cycle operational modes.

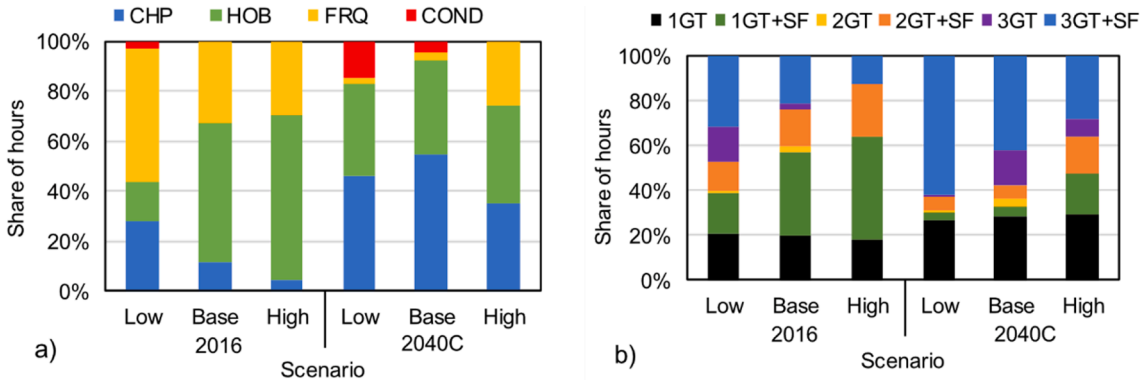

Fig. 13. The impact of fuel cost on optimal a) steam cycle mode selection and b) gas turbine and supplementary firing dispatch in 2016 and 2040C. "Low", "base" and "high" indicate the fuel/CO_2 cost level, see Table 2. Thermal flexibility = 100 000 MWh in both figures.

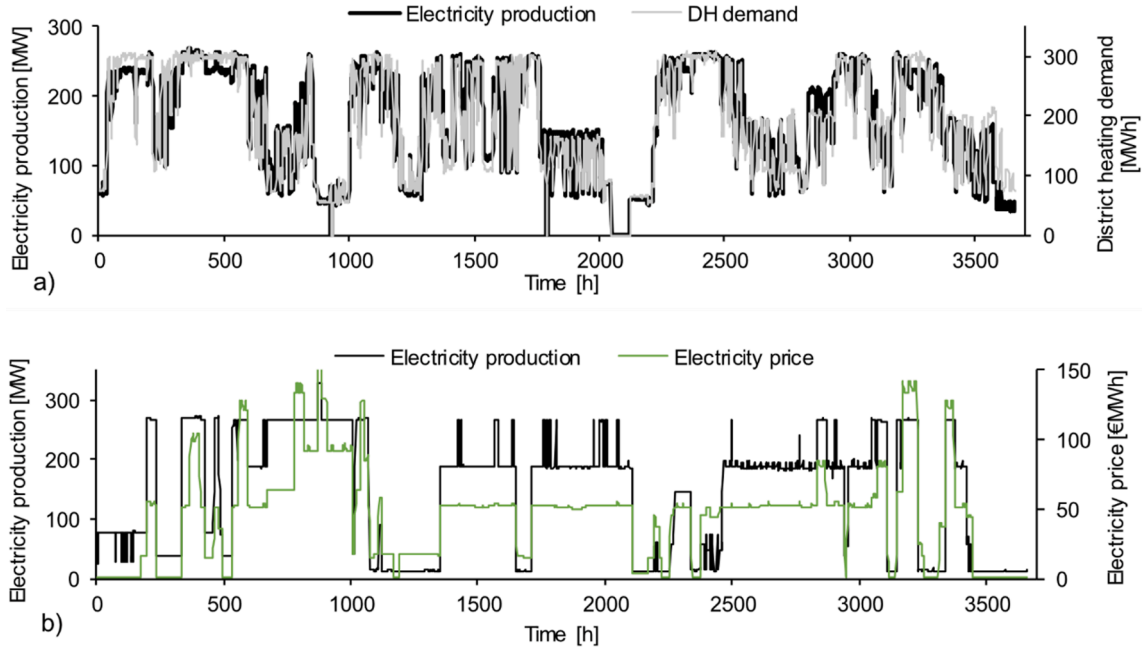

Fig. 14. Optimal plant electricity production profile (black) for the 2030C scenario with (a) no product flexibility or thermal flexibility and (b) product flexibility and 100 000 MWh thermal flexibility. The grey line in (a) shows the district heating demand (based on reference plant data), and the green line in (b) plots the electricity price.

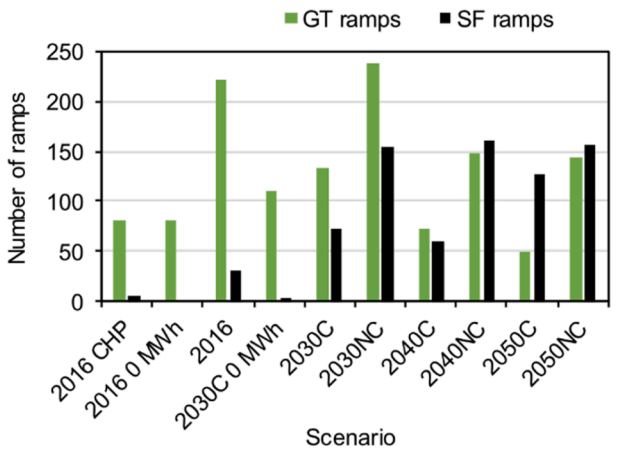

Fig. 15. The total number of ramp events for gas turbines (GT, green) and supplementary firing (SF, black) in different electricity price scenarios. Product and thermal flexibilities are available unless stated otherwise: CHP = operation without thermal and product flexibility, 0 MWh = operation without thermal flexibility. "C" and "NC" indicate scenarios with and without flexibility in sectorial coupling, respectively.

5.2.4. Combined utilization of gas turbines, supplementary firing and steam cycle modes

The combinations of optimal steam cycle modes and gas turbine/supplementary firing operation are plotted in Fig. 12 for the 2030C scenario with a) 0 MWh and b) 100 000 MWh thermal flexibility. The bubble size represents the number of hours spent in each operational mode combination. The number of bubbles indicates the number of operational combinations used by the plant. Without thermal flexibility (Fig. 12a), the plant has to operate in heat-following mode, with utilization of many operational points to match the varying heat demand, while taking advantage of market conditions when possible, by using the steam cycle modes. With thermal flexibility (Fig. 12b), fewer operational points are used and operational hours are concentrated to either low fuel-load with heat-only production in the steam cycle when electricity prices are low (1GT + HOB), or high electricity production (3GT + CHP and 3GT + CHP + SF) during high-price periods. However, although fewer operational points are utilized, it is still important that these points constitute a wide range of production levels, since the optimal operation with flexibility measures mainly includes dispatch at maximum or minimum electricity generation levels. The combined cycle might therefore benefit from the load range expansion from product flexibility, that lowers the minimum electricity generation level.

5.2.5. Impact of fuel and carbon cost

As discussed in Section 5.2.2, the operational expenditures in relation to the electricity price is a main driver for changes in operational strategies. Fig. 13 shows the impact of fuel and CO_2 cost on the optimal operation of the GTCC-CHP plant for the 2016 data and 2040C scenario, with a) the steam cycle mode distribution and b) the gas turbine/supplementary firing dispatch. For 2016 (low electricity price volatility and low average electricity price), the share of HOB operation increases with fuel cost to reduce the heat production cost, and the utilization of the steam turbine decreases. This is coupled with low-load operation of the gas turbines (1GT, 1GT + SF) up to 60% of the time to further reduce the fuel consumption. For 2040C (high electricity price volatility and high average electricity price), the higher electricity price volatility reduces the impact of the fuel cost level, with a 35–50% operation in CHP mode and 35–60% high-electricity dispatch with 3GT + SF.

5.3. Dynamic plant operation

5.3.1. Optimal plant operational patterns

The optimal GTCC-CHP plant electricity production profile is plotted in Fig. 14 for the 2030C scenario with a) no product flexibility or thermal flexibility and b) product flexibility with 100 000 MWh thermal flexibility. As indicated in Sections 5.2.2–4, the plant operation without thermal and product flexibility is adapted to follow the heat demand profile (grey line in Fig. 14a), and with the fixed power-to-heat ratio of the CHP mode, the electricity generation closely follows the heat demand variations. With thermal and product flexibility, the optimal electricity production and plant dispatch is instead dictated by the electricity price (green line in Fig. 14b), leading to a shift in operating strategy from the current practice. If product flexibility is available, but not thermal flexibility, the operating strategy involves a mix of heat-following and electricity-following operation (not shown); when electricity prices are low, the electricity generation is reduced and deviates from the heat demand profile, by operation in HOB mode together with a decreased load on gas turbines or supplementary firing, minimizing the fuel consumption while maintaining the heat generation.

Hence, the load changing pattern is closely connected to the variability of the electricity price and/or heat demand. However, the heat demand varies in diurnal and seasonal patterns, governed by air temperature and social factors, with slower dynamics than the electricity price, which varies in steps according to the energy-only market. The electricity price is, thus, more likely to initiate steep ramps in plant production than the heat demand.

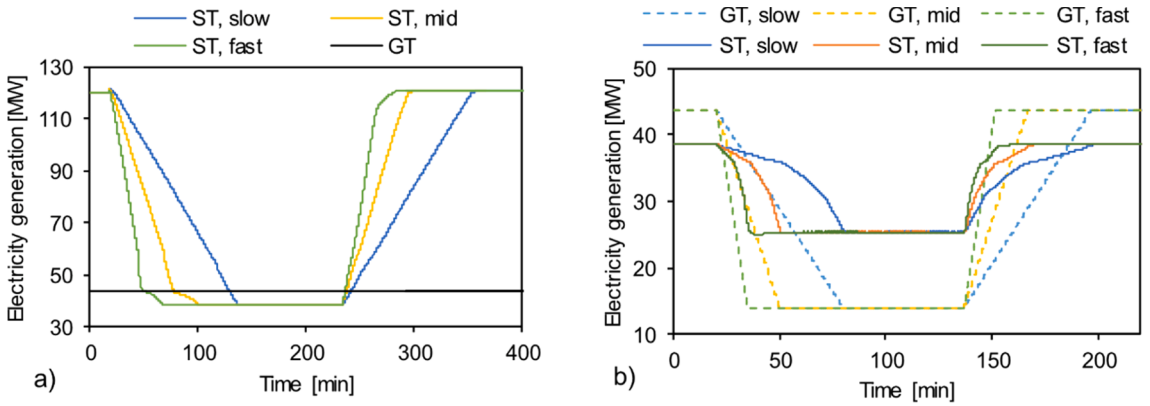

Fig. 16. Simulated electricity generation responses from the steam turbine (ST) and one gas turbine (GT) for (a) supplementary firing ramp cases, and (b) gas turbine ramp cases. The ramp cases are specified in Table 2. Note the different scales on the x-axes.

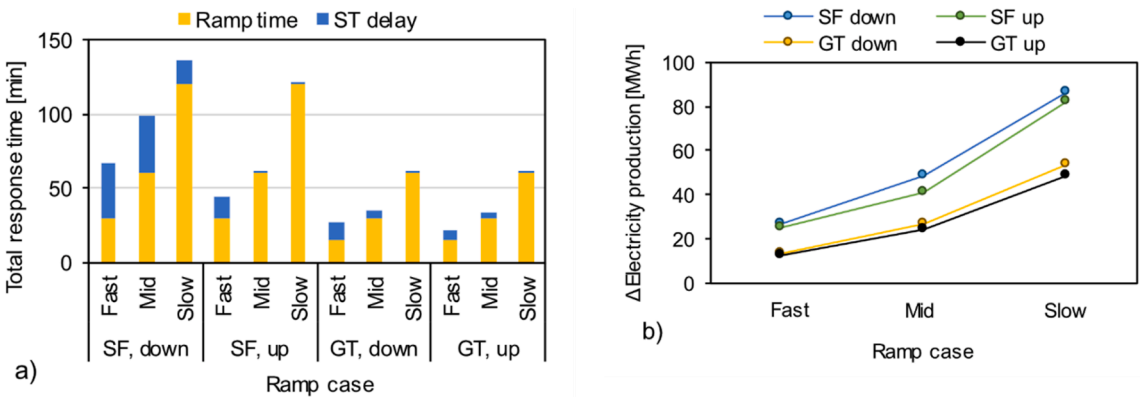

Fig. 17. (a) Total electricity generation response time for the three ramp cases simulated (Table 3), with up- and down-ramps considered separately. SF = supplementary firing, GT = gas turbine, ST = steam turbine. (b) Total plant (three gas turbines and steam turbine) absolute difference in electricity production for the three ramp cases, calculated from Eq. (2).

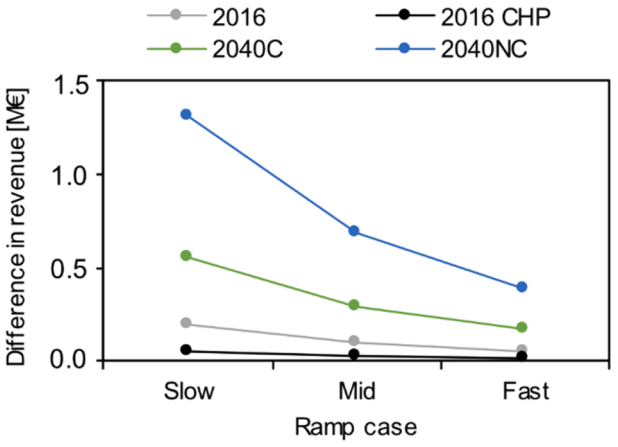

Fig. 18. Estimated annual difference in revenue, comparing static and dynamic plant operation for four electricity price scenarios. Thermal and product flexibilities are available except in 2016 CHP (no product or thermal flexibility). The exact values are given in Appendix D.

Fig. 15 shows the total number of ramp events in different electricity price scenarios. A gas turbine (GT) ramp is here defined as a load change of at least 50% of rated power over 1 h, while a supplementary firing (SF) load change must be at least 75% of the maximum SF load, over 2 h. The number of ramps varies between scenarios, both for GTs and SF; but the number of ramps is generally higher in NC-scenarios (without load flexibility in sector collaborations) that in C-scenarios, highlighting that if the electricity system flexibility from demand side management, sector coupling or storages is low, the dispatchable generation units operate more flexibly instead.

5.3.2. *Dynamic ramp simulation responses*

This section considers the dynamic part of operational flexibility, the ramp rate, and its impact on the plant's electricity production during load changes. The three ramp cases, (fast, mid and slow, Table 2) are simulated with the dynamic process model. Fig. 16 plots the dynamic electricity generation responses from the steam turbine and one of the three gas turbines for a) supplementary firing ramps, and b) gas turbine ramp cases. The gas turbines run at constant full load in Fig. 16a, independent of the supplementary firing ramp case, hence the flat response signal.

Fig. 17a plots the total electricity generation response time for the plant, considering up- and down-ramping of supplementary firing and gas turbines, as well as the steam turbine response delay time (99% settling [53]). The exact values are given in Appendix D. The steam turbine response delay compared to the supplementary firing and gas turbine response is less than 2.5 min for gas turbine ramps, and up to 39 min for supplementary firing ramps. Thus, the total plant response time is in some of the cases longer than the hourly timescale applicable to the optimization model. All supplementary firing up-ramp cases have total response times longer than 60 min, although the main part of the load change is obtained at a shorter response time (Fig. 16). All gas turbine ramp cases are achievable within one hour.

Fig. 17b shows the difference in electricity production from the three gas turbines and the steam turbine, comparing dynamic and instantaneous (static plant) load changes (Eq. (2)). The exact values are given in Appendix D. The difference in production is slightly higher for down-ramps than up-ramps for both gas turbine and supplementary firing ramping, which is also seen in Fig. 16: for the down-ramps, the steam turbine responses are initially flat, causing electricity generation to remain at a higher level for a longer period of time. This is due to the initial increase in gas turbine exhaust temperature for gas turbine ramps (Fig. 7), that impacts the live steam parameters, and consequently the steam turbine electricity generation. The difference is larger for supplementary firing ramps (25–86 MWh) compared to gas turbine ramps (12–54 MWh), due to the larger change in electricity generation obtained from supplementary firing (Fig. 16).

Based on the annual number of ramp events given in Fig. 15, the annual difference in electricity production is calculated and ranges from 0.6 to 14.5 GWh for the slow ramp case, which can be compared to the annual plant electricity production from the optimization model results of 330–640 GWh. The difference in electricity production between static optimization model assumptions and dynamic operation is, thus, less than 5% of the annual production, and might be considered negligible.

5.3.3. *Impact of ramp rate on plant revenue*

Based on the estimated number of ramps in each electricity price scenario (Fig. 15), Fig. 18 shows the difference in annual revenue between static operation (as assumed in the optimization model) and dynamic operation (Eqs. (3) and (4)), for four electricity price scenarios and the three ramp cases. The corresponding results for the remaining electricity price scenarios are given in Appendix D. The revenue difference calculation is based on an approximate peak electricity price level based on the electricity price distributions, assuming that ramp events would occur when the electricity price increases to, or decreases from, peak level.

The differences in revenue are between 0.05 and 1.4 M€, depending on scenario and ramp case, which can be compared to the revenue increases from product and/or thermal flexibility plotted in Fig. 9, that

range from 0.2 to 14 M€. The ramp rate-induced impact on the revenue might, thus, be considered marginal; in particular for scenarios with low price volatility and without flexibility measures (e.g. 2016 and 2016 CHP). For electricity price scenarios with high volatility, exemplified by 2040C and 2040NC in Fig. 18, the impact on revenue is larger (up to 1.4 M€), especially for N-scenarios without flexibility in sector coupled loads where ramp events occur more frequently (Fig. 15). The revenue difference decreases by approximately 50% for a doubling of the ramp rate, e.g. by going from slow to mid ramp rate.

Thus, from an energy-only market perspective, the value of operational flexibility in terms of ramp rate is low for the GTCC-CHP plant compared to the potential value of product and/or thermal flexibility, and in particular for current market conditions. On the other hand, fast ramping could be valuable from other electricity system perspectives; for example, for participation in ancillary grid service markets, where regulating power made available on short notice is traded. The results support the assumption made for the optimization model; that the plant can be treated as static with load changes happening instantaneously, since the dynamic transition between load levels will not impact the annual revenue considerably.

6. Conclusion

An analysis of the relative impact on operation and plant revenue of system and process level flexibilities in a heat-driven cogeneration combined cycle is performed. The work proposes a flexibility categorization structure, including three types of flexibility: the operational flexibility of the fuel conversion system, product flexibility of the steam cycle with variable product ratios (heat/electricity/primary frequency response), and thermal flexibility in the district heating system; as well as a modeling framework based on process simulation and optimization models to join static, dynamic, technical and economic perspectives on flexibility. The results point to the need for methods that combine several types of models; flexibility is a diverse concept with many interpretations and applications and involves complex interactions between plant-system flexibility. This work demonstrates that coupling of different models can give complementary perspectives on the value of flexibility, approaching a holistic evaluation.

The work applies the method to a case study of a 250 MW_{el} cogeneration plant. The main conclusions from the case study are summarized in the following points:

- Product and thermal flexibility have the most significant impact on the annual plant revenue (up to 16.5 M€ revenue increase for a 250 MW_{el} plant), while ramp rate, as a form of operational flexibility, has a comparatively small impact on plant revenue (0.1–1.4 M€). Product flexibility is the most valuable in district heating systems with limited thermal flexibility (<1000 MWh), while thermal flexibility dominates the revenue increase for levels that approach seasonal heat storages. However, the value of these flexibilities is strongly connected to the electricity price volatility: high volatility yields larger increases in plant revenue, and most measures have a limited impact in the present system.
- During periods with low electricity prices, product flexibility is utilized to 1) operate the steam cycle with heat-only generation (30–50% of operational hours), thereby reducing the heat production cost; 2) deliver frequency response when the frequency response price is higher than the electricity price (10–50% of hours). For high electricity prices, conventional combined-heat-and-power-operation dominates (up to 50% of hours in future scenarios). The dispatch of gas turbines is also dependent on the electricity price.
- With thermal flexibility and high price volatility, the plant operation is shifted from the traditional heat-following operating pattern, to being governed by the electricity price profile. The operational modes used concentrate around minimum and maximum electricity generation, highlighting the importance of a wide load span, as enabled by product flexibility, with steam turbine electricity generation potential between 0 and 139% of nominal full load.

Although the results are based on a case study, the main operational trends observed might be generalizable to other heat-driven combined cycles. In sum, the operating strategies and profitability of cogeneration combined cycles are closely connected to the development of the energy system. In circumstances with increased integration of non-dispatchable power generation and electricity system volatility, plant level and thermal flexibility can be important measures for the economic viability of combined heat and power plants. Given the strong influence of the heat demand on plant operating patterns, and the potential benefits from thermal flexibility, further research that consider both the combined cycle and its district heating system context in greater detail could be pursued.

CRediT authorship contribution statement

Johanna Beiron: Conceptualization, Methodology, Investigation, Writing - original draft, Visualization. **Rubén M. Montañés:** Conceptualization, Methodology, Writing - review & editing, Supervision. **Fredrik Normann:** Conceptualization, Methodology, Writing - review & editing, Supervision, Project administration, Funding acquisition. **Filip Johnsson:** Writing - review & editing, Supervision, Funding acquisition.

Declaration of Competing Interest

The authors declare that they have no known competing financial interests or personal relationships that could have appeared to influence the work reported in this paper.

Acknowledgments

This project is financed by the Swedish Energy Agency, Energiforsk – The Swedish Energy Research Centre and Göteborg Energi AB. The authors gratefully acknowledge Göteborg Energi AB and Siemens Industrial Turbomachinery AB for providing data to the study. M.Sc Julia Björck Hansson and M.Sc Linnéa Östlund are acknowledged for their work on combined cycle process model development in Ebsilon Professional.

Appendix A. Optimization model formulation

The objective function maximizes the annual plant revenue and is given by Eq. (A.1). R is the revenue, C is the cost/price for electricity, primary frequency response, fuel, CO_2 emissions and gas turbine starts [33]. P, F, $Fuel$, are the production of electricity and frequency response and fuel consumption, Eqs. (5)–(7). n_{starts} is the total number of gas turbine starts. f_{CO2} relates the fuel consumption to CO_2 emissions.

$$\max R = \sum_t (C_{el}(t)P(t) + C_{frq}(t)F(t) - Fuel(t)(C_{fuel} + f_{CO2}C_{CO2}) - C_{start}n_{starts}) \quad (A.1)$$

(A.2)–(A.5) give the constraints for gas turbine and supplementary firing operation, that must be within maximum and minimum load levels. *GTon* and *SFon* are binary variables that indicate if, e.g., gas turbine *i* is in operation (value 1) or off (value 0) at time t. Eq. (A.3) also ensures that gas turbine loads are at least 80% of full load when supplementary firing is used.

$$GT(t,i) \leq GT_{max}GTon(t,i) \quad (A.2)$$

$$GT(t,i) \geq GT_{min}GTon(t,i) + (0.8GT_{max} - GT_{min})SFon(t,i) \quad (A.3)$$

$$SF(t,i) \leq SF_{max}SFon(t,i) \quad (A.4)$$

$$SFon(t,i) \leq GTon(t,i) \quad (A.5)$$

Although in practice, the start order of gas turbines will be varied to spread operational hours evenly; in the model, GT1 is always turned on first, followed by GT2 and GT3 (A.6). When supplementary firing is active, it must be used for all lines (gas turbine + HRSG) in operation at the time; Eqs. (A.7)–(A.9).

$$GT(t,3) \leq GT(t,2) \leq GT(t,1) \quad (A.6)$$

$$\sum_i SFon(t,i) \geq 3GTon(t,3) - 3(1 - SFon(t,1)) \quad (A.7)$$

$$\sum_i SFon(t,i) \geq 3GTon(t,3) - 3(1 - SFon(t,2)) \quad (A.8)$$

$$\sum_i SFon(t,i) \geq 2GTon(t,2) - 2(1 - SFon(t,1)) \quad (A.9)$$

The gas turbine cycling constraints are adapted from [29]; Eqs. (A.10)–(A.14). The binary variables *z* (value 1 if GT *i* is not in operation), *on* (value 1 if GT *i* is turned on at time *t*) and *off* (value 1 if GT *i* is turned off at time *t*) allow the gas turbines to be shut down, with a minimum up/down-time $T_{on/off}$; Eqs. (A.10) and (A.11). Eqs. (A.12)–(A.14) are logic equations that make sure that the gas turbines are not started and stopped in the same time step.

$$\sum_{h=t}^{t+T_{off}-1} z(h,i) \geq off(t,i)T_{off} \quad (A.10)$$

$$\sum_{h=t}^{t+T_{on}-1} GTon(h,i) \geq on(t,i)T_{on} \quad (A.11)$$

$$GTon(t,i) + z(t,i) = 1 \quad (A.12)$$

$$on(t,i) + off(t,i) = 1 \quad (A.13)$$

$$on(t,i) - off(t,i) = GTon(t,i) - GTon(t-1,i) \quad (A.14)$$

Only one steam cycle mode can be in operation at time *t*, as expressed by the binary variable *y* that represents the arcs from node *S* (see Fig. 6) to product nodes *j*; Eq. (A.15). The energy flow, *x*, from node *S* to product node j is restricted by a maximum capacity, S_{max}; Eq. (A.16). Energy balances for all nodes are given, e.g. Eq. (A.17); all incoming flows in arcs from nodes *j* to node *k* must equal the outgoing flows from node *k* to nodes *l*.

$$\sum_j y(t,S,j) = 1 \quad (A.15)$$

$$x(t,S,j) \leq S_{max}y(t,S,j) \quad (A.16)$$

$$\sum_j x(t,j,k) = \sum_l x(t,k,l) \quad (A.17)$$

The heat supplied to the district heating network, Q_s, must equal the demand, Q_d, every hour *t* and summed for the entire heat-generation season; Eqs. (A.18) and (A.19). If thermal flexibility is used to load shift heat production, the difference between the heat produced (*x(t,q,DH)*) and the heat supplied can be buffered by the heat storage variable *L*, whose storage level must be lower or equal to the maximum capacity; Eqs. (A.20) and (A.21). The thermal flexibility is, thus, modeled using a simplified energy balance equation.

$$Q_s(t) = Q_d(t) \quad (A.18)$$

$$\sum_t Q_s(t) = \sum_t Q_d(t) \quad (A.19)$$

$$\sum_q x(t,q,DH) = L(t) - L(t-1) + Q_s(t) \quad (A.20)$$

$$L(t) \leq L_{max} \tag{A.21}$$

Appendix B. Dynamic model transient validation responses

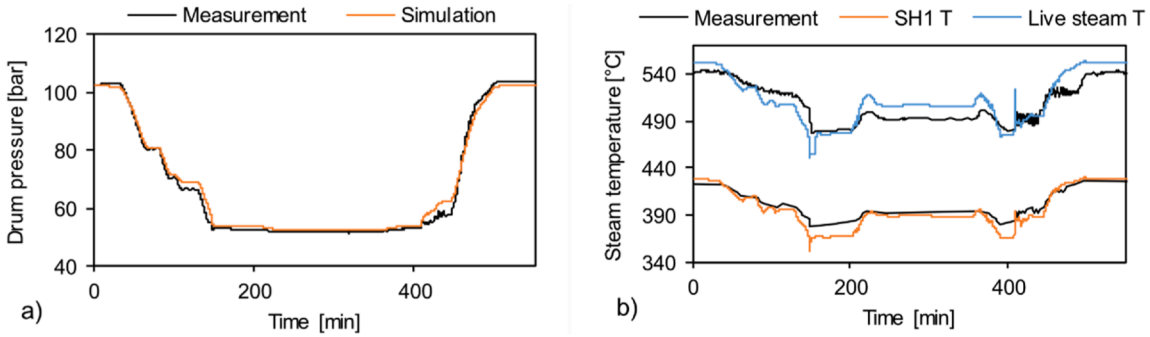

Fig. B.1. Transient validation results with simulated responses (orange and blue) and reference plant measurements (black), for a) steam drum pressure and (b) live steam and superheater 1 (SH1) outlet temperatures.

Fig. B.1 shows additional simulated responses of HRSG process variables compared to measurements from reference plant, for validation of the dynamic process model with transient data.

Appendix C. Additional dispatch optimization results

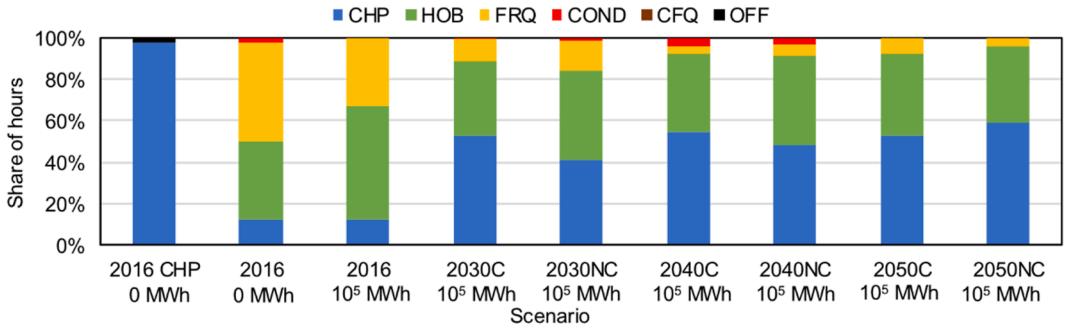

Fig. C.1. Optimal steam cycle mode selections for the 2016–2050 scenarios. CHP = operation without product flexibility. The thermal flexibility available is given in MWh.

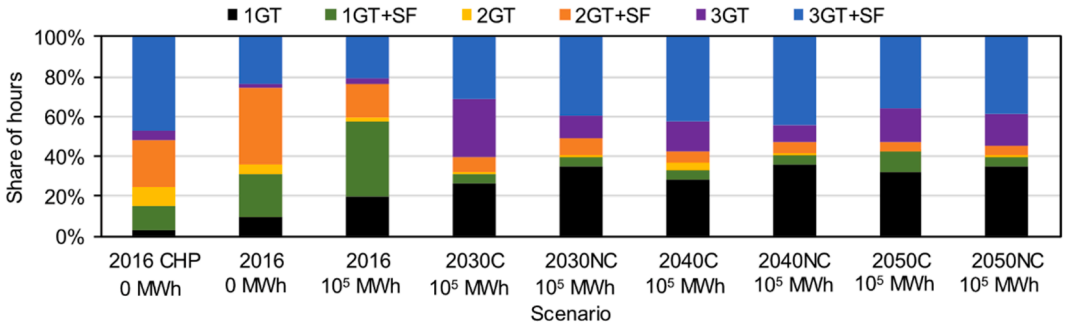

Fig. C.2. Optimal utilization of gas turbines and supplementary firing for the 2016–2050 scenarios. CHP = operation without product flexibility. The thermal flexibility available is given in MWh.

Figs. C.1 and C.2 present the optimal utilization of the steam cycle product flexibility and the gas turbines and supplementary firing dispatch for the seven electricity price scenarios.

Appendix D. Additional ramp rate results

Table D.1
Electricity production difference of fast, mid and slow ramp rates, compared to the static plant assumption; and the steam turbine delay time compared to gas turbine responses, for gas turbine and supplementary firing up- and down-ramps.

		Gas turbine production		Steam turbine production		Total plant production		Steam turbine delay compared to GT	
Ramp case		ΔP [MW]	ΔP_{ramp} [MWh]	ΔP [MW]	ΔP_{ramp} [MWh]	ΔP [MW]	ΔP_{ramp} [MWh]	95% settled [min]	99% settled [min]
SF, down	*Fast*	0	0	81,3	26,5	81,3	26,5	28,0	36,3
	Mid	0	0	81,3	48,4	81,3	48,4	26,2	38,9
	Slow	0	0	81,3	86,8	81,3	86,8	16,5	16,6
SF, up	*Fast*	0	0	81,3	−24,8	81,3	−24,8	7,0	14,4
	Mid	0	0	81,3	−41,0	81,3	−41,0	0,7	1,2
	Slow	0	0	81,3	−81,9	81,3	−81,9	−0,2	0,2
GT, down	*Fast*	29,8	3,7	13,3	2,4	102,7	13,5	1,0	12,2
	Mid	29,8	7,4	13,3	4,7	102,7	26,9	1,4	4,9
	Slow	29,8	14,9	13,3	9,3	102,7	54,0	2,4	1,0
GT, up	*Fast*	29,8	−3,7	13,3	−1,2	102,7	−12,3	0,9	6,8
	Mid	29,8	−7,4	13,3	−2,2	102,7	−24,4	0,4	3,2
	Slow	29,8	−14,9	13,3	−4,3	102,7	−49,0	−0,4	0,8

Table D.2
Estimation of the annual number of ramps, electricity production difference, and revenue difference from electricity sales, comparing static and dynamic plant operation, for the electricity price scenarios.

Scenario	2016 CHP	2016 0 MWh	2016	2030C 0 MWh	2030C	2030NC	2040C	2040NC	2050C	2050NC
No. of ramps										
GT, up	45	43	110	56	66	118	36	73	24	70
GT, down	37	38	111	55	68	120	37	74	26	73
SF, up	4	0	10	2	33	70	30	80	62	78
SF, down	2	0	20	2	39	85	30	80	66	78
Production difference [GWh]										
Slow	1,1	0,6	4,0	1,1	7,0	14,7	5,6	14,5	11,1	14,1
Mid	0,6	0,3	2,1	0,6	3,7	7,7	2,9	7,7	5,9	7,5
Fast	0,3	0,1	1,2	0,3	2,1	4,4	1,7	4,4	3,4	4,3
Peak-level electricity price [€/MWh]	50	50	50	80	80	80	100	90	100	100
Total ΔR [M€]										
Slow	0,05	0,03	0,20	0,09	0,56	1,17	0,56	1,30	1,11	1,41
Mid	0,03	0,01	0,10	0,05	0,29	0,62	0,29	0,69	0,59	0,75
Fast	0,02	0,01	0,06	0,02	0,17	0,35	0,17	0,39	0,34	0,43

Table D.1 presents the electricity production difference between static and dynamic plant operation for the gas turbine and steam turbine, for the three ramp rate cases and up- and down-ramps. The delay of the steam turbine response compared to the gas turbine response is also included, for 95% and 99% settling [53]. Table D.2 gives the number of ramp events per electricity scenario, the corresponding annual electricity production difference and the resulting revenue difference, ΔR.

References

[1] Kondziella H, Bruckner T. Flexibility requirements of renewable energy based electricity systems – a review of research results and methodologies. Renew Sustain Energy Rev 2016;53:10–22. https://doi.org/10.1016/j.rser.2015.07.199.

[2] Olsen KP, Zong Y, You S, Bindner H, Koivisto M, Gea-Bermúdez J. Multi-timescale data-driven method identifying flexibility requirements for scenarios with high penetration of renewables. Appl Energy 2020;264:114702. https://doi.org/10.1016/j.apenergy.2020.114702.

[3] IEA (International Energy Agency). Harnessing Variable Renewables, A Guide to the Balancing Challenge; 2011. doi:612011171P1.

[4] Agora Energiewende. Flexibility in thermal power plants - With a focus on existing coal-fired power plants; 2017.

[5] Brouwer AS, van den Broek M, Seebregts A, Faaij A. Operational flexibility and economics of power plants in future low-carbon power systems. Appl Energy 2015;156:107–28. https://doi.org/10.1016/j.apenergy.2015.06.065.

[6] Kubik ML, Coker PJ, Barlow JF. Increasing thermal plant flexibility in a high renewables power system. Appl Energy 2015;154:102–11. https://doi.org/10.1016/j.apenergy.2015.04.063.

[7] Eser P, Singh A, Chokani N, Abhari RS. Effect of increased renewables generation on operation of thermal power plants. Appl Energy 2016;164:723–32. https://doi.org/10.1016/j.apenergy.2015.12.017.

[8] Gonzalez-Salazar MA, Kirsten T, Prchlik L. Review of the operational flexibility and emissions of gas- and coal-fired power plants in a future with growing renewables. Renew Sustain Energy Rev 2018;82:1497–513. https://doi.org/10.1016/j.rser.2017.05.278.

[9] Beiron J, Montañés RM, Normann F, Johnsson F. Combined heat and power operational modes for increased product flexibility in a waste incineration plant. Energy 2020;202:117696. https://doi.org/10.1016/j.energy.2020.117696.

[10] Hentschel J, Babić U, Spliethoff H. A parametric approach for the valuation of power plant flexibility options. Energy Rep 2016;2:40–7. https://doi.org/10.1016/j.egyr.2016.03.002.

[11] Nuytten T, Claessens B, Paredis K, Van Bael J, Six D. Flexibility of a combined heat and power system with thermal energy storage for district heating. Appl Energy 2013;104:583–91. https://doi.org/10.1016/j.apenergy.2012.11.029.

[12] Pini Prato A, Strobino F, Broccardo M, Parodi GL. Integrated management of cogeneration plants and district heating networks. Appl Energy 2012;97:590–600. https://doi.org/10.1016/j.apenergy.2012.02.038.

[13] Vandermeulen A, van der Heijde B, Helsen L. Controlling district heating and cooling networks to unlock flexibility: a review. Energy 2018;151:103–15. https://doi.org/10.1016/j.energy.2018.03.034.

[14] Zheng J, Zhou Z, Zhao J, Wang J. Integrated heat and power dispatch truly utilizing thermal inertia of district heating network for wind power integration. Appl Energy 2018;211:865–74. https://doi.org/10.1016/j.apenergy.2017.11.080.

[15] Wang J, You S, Zong Y, Træholt C, Dong ZY, Zhou Y. Flexibility of combined heat and power plants: a review of technologies and operation strategies. Appl Energy 2019;252. https://doi.org/10.1016/j.apenergy.2019.113445.
[16] Cáceres I, Nord L, Montañés R. Flexible operation of combined cycle gas turbine power plants with supplementary firing. J Power Technol 2018;98:188–97.
[17] Richter M, Oeljeklaus G, Görner K. Improving the load flexibility of coal-fired power plants by the integration of a thermal energy storage. Appl Energy 2019; 236:607–21. https://doi.org/10.1016/j.apenergy.2018.11.099.
[18] Nord LO, Montañés RM. Compact steam bottoming cycles: model validation with plant data and evaluation of control strategies for fast load changes. Appl Therm Eng 2018;142:334–45.
[19] Rúa J, Nord LO. Optimal control of flexible natural gas combined cycles with stress monitoring: linear vs nonlinear model predictive control. Appl Energy 2020;265: 114820. https://doi.org/10.1016/j.apenergy.2020.114820.
[20] Benato A, Stoppato A, Mirandola A. Dynamic behaviour analysis of a three pressure level heat recovery steam generator during transient operation Combined Cycle Gas Turbine plant. Energy 2015;90:1595–605. https://doi.org/10.1016/j.energy.2015.06.117.
[21] Benato A, Stoppato A, Mirandola A, Destro N, Bracco S. Superheater and drum lifetime estimation: an approach based on dynamic analysis. J Energy Resour Technol 2018;139:1–7. https://doi.org/10.1115/1.4035020.
[22] Angerer M, Kahlert S, Spliethoff H. Transient simulation and fatigue evaluation of fast gas turbine startups and shutdowns in a combined cycle plant with an innovative thermal buffer storage. Energy 2017;130:246–57. https://doi.org/10.1016/j.energy.2017.04.104.
[23] Stoppato A, Mirandola A, Meneghetti G, Lo CE. On the operation strategy of steam power plants working at variable load: technical and economic issues. Energy 2012;37:228–36. https://doi.org/10.1016/j.energy.2011.11.042.
[24] Montañés RM, Gardarsdóttir SÓ, Normann F, Johnsson F, Nord LO. Demonstrating load-change transient performance of a commercial-scale natural gas combined cycle power plant with post-combustion CO2 capture. Int J Greenh Gas Control 2017;63:158–74. https://doi.org/10.1016/j.ijggc.2017.05.011.
[25] Göransson L, Goop J, Odenberger M, Johnsson F. Impact of thermal plant cycling on the cost-optimal composition of a regional electricity generation system. Appl Energy 2017;197:230–40. https://doi.org/10.1016/j.apenergy.2017.04.018.
[26] Garðarsdóttir S, Göransson L, Normann F, Johnsson F. Improving the flexibility of coal-fired power generators: impact on the composition of a cost-optimal electricity system. Appl Energy 2018;209:277–89. https://doi.org/10.1016/j.apenergy.2017.10.085.
[27] Wogrin S, Galbally D, Ramos A. CCGT unit commitment model with first-principle formulation of cycling costs due to fatigue damage. Energy 2016;113:227–47. https://doi.org/10.1016/j.energy.2016.07.014.
[28] Hermans M, Bruninx K, Delarue E. Impact of CCGT start-up flexibility and cycling costs toward renewables integration. IEEE Trans Sustain Energy 2018;9:1468–76. https://doi.org/10.1109/TSTE.2018.2791679.
[29] Romanchenko D, Odenberger M, Göransson L, Johnsson F. Impact of electricity price fluctuations on the operation of district heating systems: a case study of district heating in Göteborg, Sweden. Appl Energy 2017;204:16–30. https://doi.org/10.1016/j.apenergy.2017.06.092.
[30] Glensk B, Madlener R. The value of enhanced flexibility of gas-fired power plants: a real options analysis. Appl Energy 2019;251:113–25. https://doi.org/10.1016/j.apenergy.2019.04.121.
[31] Mikkola J, Lund PD. Modeling flexibility and optimal use of existing power plants with large-scale variable renewable power schemes. Energy 2016;112:364–75. https://doi.org/10.1016/j.energy.2016.06.082.
[32] MacDowell N, Staffell I. The role of flexible CCS in the UK's future energy system. Int J Greenh Gas Control 2016;48:327–44.
[33] Göransson L, Lehtveer M, Nyholm E, Taljegard M, Walter V. The benefit of collaboration in the North European electricity system transition — system and sector perspectives. Energies 2019;12:4648. https://doi.org/10.3390/en12244648.
[34] Eurostat. Energy statistics - prices of natural gas and electricity 2020. https://ec.europa.eu/eurostat/en/web/energy/data/database?p_p_id=NavTreeportletprod_WAR_NavTreeportletprod_INSTANCE_QAMy7Pe6HwI1&p_p_lifecycle=0&p_p_state=normal&p_p_mode=view&p_p_col_id=column-2&p_p_col_count=1.
[35] Sandbag. Carbon price viewer 2020. https://sandbag.org.uk/carbon-price-viewer/.
[36] Pihl E, Johnsson F, Thunman H. Biomass retrofitting a natural gas-fired plant to a Hybrid Combined Cycle (HCC). In: ECOS 2009 - 22nd Int Conf Effic Cost, Optim Simul Environ Impact Energy Syst; 2009. p. 2163–76.
[37] Taljegard M, Göransson L, Odenberger M, Johnsson F. Electric vehicles as flexibility management strategy for the electricity system - a comparison between different regions of Europe. Energies 2019;12:2597. https://doi.org/10.3390/en12132597.
[38] Vogl V, Åhman M, Nilsson LJ. Assessment of hydrogen direct reduction for fossil-free steelmaking. J Clean Prod 2018. https://doi.org/10.1016/j.jclepro.2018.08.279.
[39] Nordpool. Historical Market Data; 2020. https://www.nordpoolgroup.com/historical-market-data/.
[40] Svenska Kraftnät. Primärreglering; 2020. https://mimer.svk.se/PrimaryRegulation/PrimaryRegulationIndex.
[41] Montañés RM, Flø NE, Nord LO. Dynamic process model validation and control of the amine plant at CO2 technology centre Mongstad. Energies 2017;10:1527. https://doi.org/10.3390/en10101527.
[42] EBSILON Professional; 2020. https://www.steag-systemtechnologies.com/en/products/ebsilon-professional/.
[43] Cooke DH. On prediction of off-design multistage turbine pressures by Stodola's ellipse. Trans ASME 1985;107:596–606.
[44] Hansson Björck J, Östlund L. Opportunities for flexible operation of a combined heat and power plant in power systems with volatile electricity prices (MSc Thesis). Chalmers University of Technology; 2019.
[45] Modelica and the Modelica Association; 2020. https://www.modelica.org/.
[46] Dymola Systems Engineering; 2020. https://www.3ds.com/products-services/catia/products/dymola/.
[47] Modelon Thermal Power Library; 2020. https://www.modelon.com/library/thermal-power-library/.
[48] Beiron J, Montañés RM, Normann F, Johnsson F. Dynamic modeling for assessment of steam cycle operation in waste-fired combined heat and power plants. Energy Convers Manag 2019;198:111926. https://doi.org/10.1016/j.enconman.2019.111926.
[49] Gardarsdóttir S, Montañés RM, Normann F, Nord LO, Johnsson F. Effects of CO_2-absorption control strategies on the dynamic performance of a supercritical pulverized-coal-fired power plant. Ind Eng Chem Res 2017;56:4415–30. https://doi.org/10.1021/acs.iecr.6b04928.
[50] Chen C, Zhou Z, Bollas GM. Dynamic modeling, simulation and optimization of a subcritical steam power plant. Part I: Plant model and regulatory control. Energy Convers Manag 2017;145:324–34. https://doi.org/10.1016/j.enconman.2017.04.078.
[51] Montañés RM. Transient performance of combined cycle power plant with absorption based post-combustion CO2 capture: dynamic simulations and pilot plant testing (PhD Thesis). Norwegian University of Science and Technology; 2018.
[52] Shin JY, Jeon YJ, Maeng DJ, Kim JS, Ro ST. Analysis of the dynamic characteristics of a combined-cycle power plant. Energy 2002;27:1085–98.
[53] Seborg DE, Edgar TF, Mellichamp DA, Doyle FJ. Process dynamics and control. 3rd ed. John Wiley & Sons; 2011.